University of Natural Resources and Life Sciences
Department of Civil Engineering and Natural Hazards

Institute of Mountain Risk Engineering
Peter Jordan Str. 82 Tel.: +43-1-47654-4350
A-1190 WIEN Fax: +43-1-47654-4390

IAN REPORT 171

Physical Modeling of the Cougar Creek Debris Flood Retention Structure

Vienna, February 2016

IAN Report 171:

Physical Modeling of the

Cougar Creek Debris Flood Retention Structure

Projektleitung: Univ. Prof. Dipl.-Ing. Dr. Hübl Johannes

Mitarbeiter: Falkensteiner Martin

Dipl.-Ing. Dr. Chiari Michael

Iliadis Marie

University of Natural Resources and Life Sciences

Department of Civil Engineering and Natural Hazards

Institute of Mountain Risk Engineering

Peter Jordan Str. 82 Tel.: +43-1-47654-4350

A-1190 WIEN Fax: +43-1-47654-4390

Reference: HÜBL, J., FALKENSTEINER, M., CHIARI, M., ILIADIS, M. (2016): Physical Modeling of the Cougar Creek Debris Flood Retention Structure; IAN Report 171, Department of Civil Engineering and Natural Hazards, University of Natural Resources and Life Sciences – Vienna (unpublished)

Vienna, February 2016

Contents

Introduction

Cougar Creek is part of the Mountain Creek Hazard Mitigation Program. After the debris-flood event in June 2013, establishing long-term mitigation became a priority for the Town of Canmore in order to avoid another catastrophic situation. Indeed, this last mountain hazard caused severe damages in the Cougar Creek catchment and on the alluvial fan. Moreover, a part of the Trans-Canadian Highway and Canadian-Pacific Railway was destroyed, breaking connections between Banff (West of Canmore) and Calgary (BGC ENGINEERING Ltd., 2014). The short-term mitigation was initiated early 2014 and completed in May 2014, one year after the devastating event (CANMORE, 2015a), including excavations of the creek channel, cleaning out debris aggraded during the debris-flood of 2013, construction of channel bed protection and a debris net , *etc*.

Many scientific studies were conducted on Cougar Creek, mainly about geomorphology, hydro - climate and watershed. For long-term mitigation a debris flood retention structure was recommended following an option analysis and evaluation phase. ALPINFRA CONSULTING + ENGINEERING GMBH and Canadian Hydrotech Corp. are the main consultants on the project.

To support the process of planning, hydraulic experiments on a physical scale model were performed at the Institute of Mountain Risk Engineering of University of Natural Resources and Life Sciences in Vienna.

Scope of the project was:

- hydraulic optimization of the outlet channel geometry.
- optimizations of roughness in the outlet channel;
- investigations on the effect of different throttle designs;
- optimization of the gravel rake shape;
- investigations on sediment deposition in the culvert;
- observations of the location of a hydraulic jump and
- investigations on deposition and erosion of sediment up- and downstream of the debris flood retention structure.

1 Model Setup

1.1 Froude scaling

In order to transfer all the processes and conclusions between the model and reality, mechanical similarity, which comprises geometric, kinematic, and dynamic similarity, has to be fulfilled (Preissler et al. 1989). In open channel flows, the flowing medium is water, which has a very low Newtonian viscosity. For phenomena where gravity and inertial forces are dominant and effects of remaining forces such as kinematic viscosity are small, Froude scaled models are preferred. In order to keep unavoidable errors small, the geometrical scaling factor should be kept as small as possible (i.e. the physical model should be as large as possible). The scale for the Cougar Creek model was chosen to equal 1:30.

In continuum mechanics, the Froude number (Fr) is a dimensionless number defined as the ratio of the flow inertia to the external field. Named after William Froude, the Froude number is based on the speed–length ratio as defined:

$$Fr = \frac{v_0}{\sqrt{g * h}}$$

where v_0 is a characteristic flow velocity, g is the acceleration due to gravity, and h is a characteristic length (PREIßLER and BOLLRICH, 1985). Equality in Fr in model and full scale will ensure that gravity forces are correctly scaled.

In Table 1 the scaling ratio along for different physical units is given by λ, which is the scaling factor for Froude similarity.

Table 1: Scaling ratio along Froude similarity law.

description	*symbol*	*scale function (Fr)*
length	l	λ
acceleration	b	λ^0
pressure	p	λ
speed	v	$\lambda^{1/2}$
discharge	q	$\lambda^{5/2}$
time	t	$\lambda^{1/2}$

1.2 Construction of the model

For the experiments in the laboratory of the Institute of Mountain Risk Engineering a Froude-scaled model with a physical scale of 1/30 was built.

Due to a limited width of the laboratory a 30m wide section of the retention structure with the bottom outlet channel in the center was represented by the model. The length of the upstream channel bed was limited to 115m in natural dimensions. For the upstream channel bed an average inclination (3.5 %) of the last 165m upstream was used. The geometric design of the dam was planned according to specifications provided by **alp**infra. The inclination at the footprint of the retention structure was 4.37 %. The inclination of the upstream embankment dam also followed the information from **alp**infra, but neglecting the access road. After all, the inclination from the lowest to the highest point of the dam cross section was used (38.1 %). To provide a better insight into the process of the tunnel discharge, the downstream surface of the model was not installed for the first tests. It was added eventually for the 'overflow' (2.1.1.4) tests in the last stage of the modeling.

The overall dimensions of the Cougar Creek test setup reached a length of 14m and a width of 3m, including:

- The water supply with water reservoir, Thomson weir and bypass (3.05 m length).
- The central model with riverbed section and dam structure (8.9 m length).
- The section for the stilling basin and erosion area (1.6 m length).
- The filter basin, partly placed below the erosion area (1.24 m length, 0.48 m overlapping).

A conveyor belt was used to add bedload material.

1.2.1 Water supply

The configuration of our laboratory includes a 27 m^3 sub level water basin (see Figure 7). A circulating pump (type: Grundfos - CLM 150-271-18.5 A-F-A-BBU) brings up the water (up to 50 l/s) and fills the so-called 'Thomson Basin'.

Subsequent to the Thomson Basin is an intermediate basin with bypass, which allows to suddenly stop the discharge in the model (Figure 1).

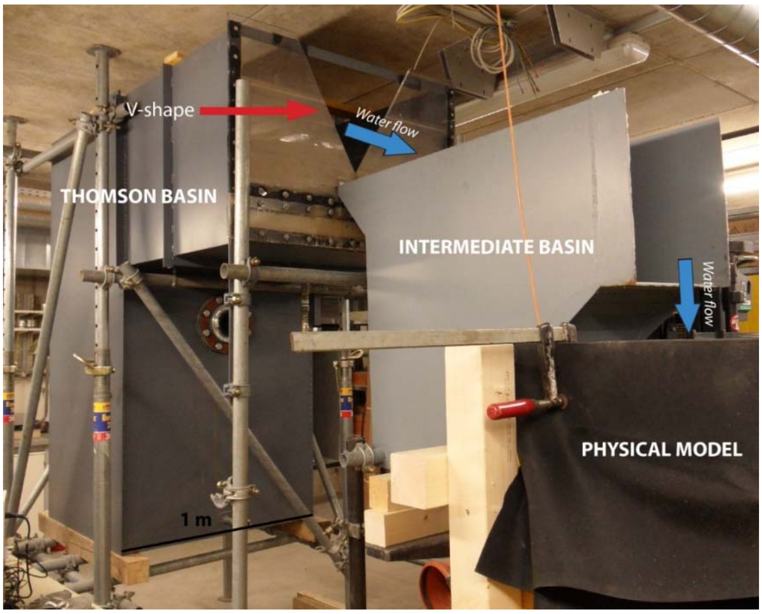

Figure 1: Water supply installations.

1.2.2 Central model

The main model was based on 10 reinforced 'U-profiles' made out of 10 x 10 cm square shaped timber. The 'U-profiles' had an inner width of 120 cm and a height of 150 cm (see Figure 9).

The profiles were placed in a line with a distance of 100 cm from each other and horizontal leveled. A vertically placed raster framework out of a three-layer sheeting (company: doka) was placed on the base structure, following the specified inclinations for the channel bed and the embankment dam structure (see Figure 2). Sheeting boards (1 m wide) were placed on that framework, providing the base layer for the dam structure and a sealing foil.

Further, 1.5 m wide three-layer boards, fixed vertically to the left and right and the upstream head end of the model, flanked the bottom construction. The sidewalls were supported by the above-mentioned u-profiles in a vertical, and 20 x 8 cm H-beam timber in a horizontal direction. The model of the dam structure was placed in this channel, so the retention basin was formed. The foundation was then covered with an impermeable foil out of EPDM-material.

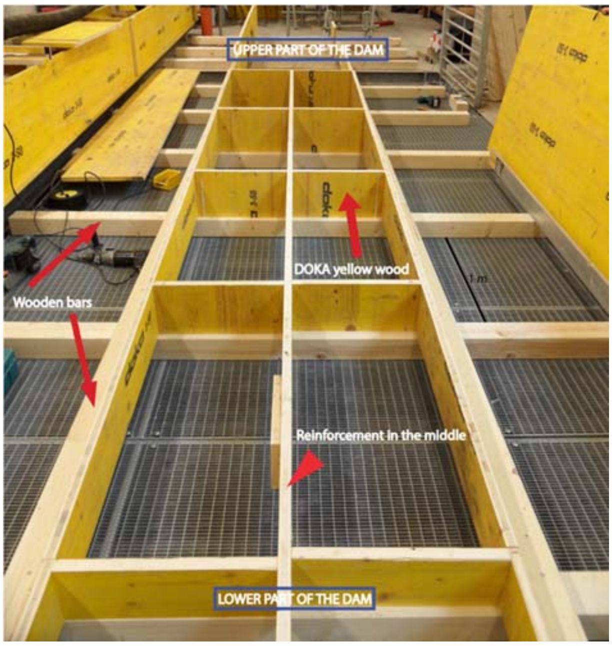

Figure 2: Base framework of the model (Iliadis, 2015).

Additional sheeting boards for further installations were placed on the sealing layer. An additional basin with scum baffle (breaking the velocity of the inflow) was fixed on the boards, placed on the channel bed section. The channel roughness was placed on those boards too. The boards at the upstream slope of the embankment dam supported the installation of the throttle, the different inlet designs and rakes.

1.2.2.1 Dam slopes

The upstream dam slope showed a rectangular, rake-covered bypass channel, with a width of 33.3 cm and a depth of 8.33 cm, including the rake construction. If the lower rake structure is clogged, water can pass through this bypass and will discharge through into the outlet channel (see Figure 3). This ensures a controlled discharge downstream the dam.

For the downstream face of the dam it was needed to install an adequate roughness, corresponding to riprap in natural dimensions (see Figure 4). The inclination of 30° follows the requirements of **alp**infra. The design of the transition reach between dam foot and stilling basin was adapted during the project.

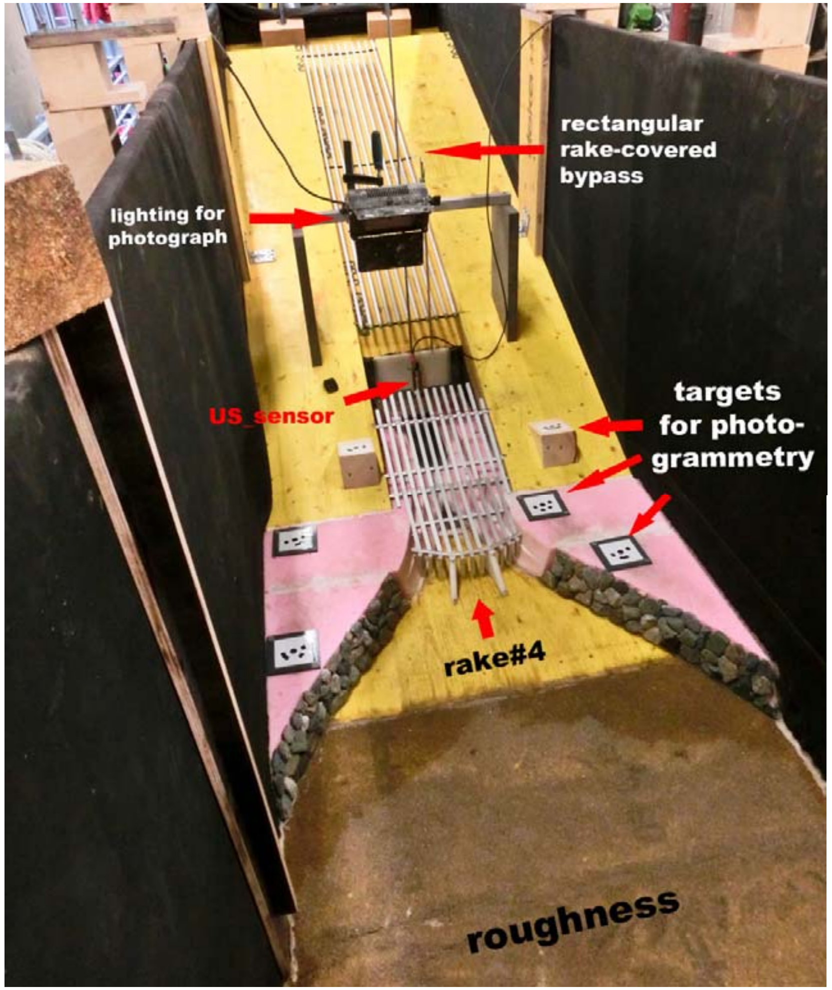

Figure 3: Upstream dam surface, rake and inlet design.

Figure 4: Downstream dam structure.

1.2.2.2 Culvert

The culvert channel was designed as a sealed U-profile, one sidewall made out of transparent acrylic plastic. With a length of 4.34 m it reached from the throttle to the end of the dam and followed the inclination of the dam base. This basic structure enabled the installation of different culvert designs and facilitated observations through the transparent outlet (see Figure 10).

1.2.2.3 Inlet design

A rectangular cutting in the dam structure (horizontal distance of 78 cm from the intersection of the upstream dam surface and the channel bed; width of 33.3 cm) incorporated the culvert inlet and the throttle structure.

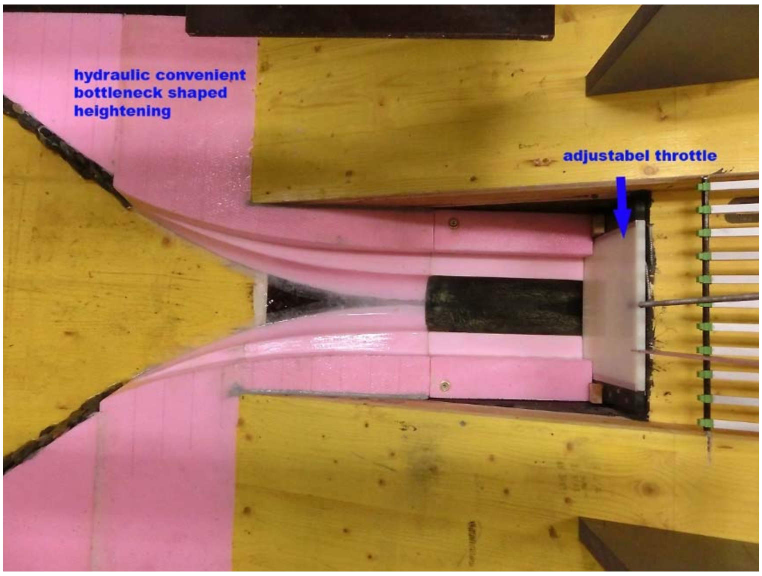

Figure 5: Inlet design and throttle.

Upstream of the inlet a hydraulically convenient bottleneck was shaped to minimize energy losses. Along this narrowing the slope of the side walls was 4V:1H at the stone-pitched bottleneck (height of 10 cm) and then transitions to the circular shaped outlet channel design. This design was constructed by shaping insulation boards and adding riprap (according to the physical scale of the model) in the section upstream of the rake structure (see Figure 5).

1.2.2.4 Throttle

The throttle was designed as vertical adjustable slide (27 x 24 x 1.2 cm) in front of the culvert inlet (see Figure 6). The overlapping design guaranteed a sealed performance. A measuring scale with vernier supported the detection of accurate adjustments. For testing different throttle designs the throttle could be changed easily.

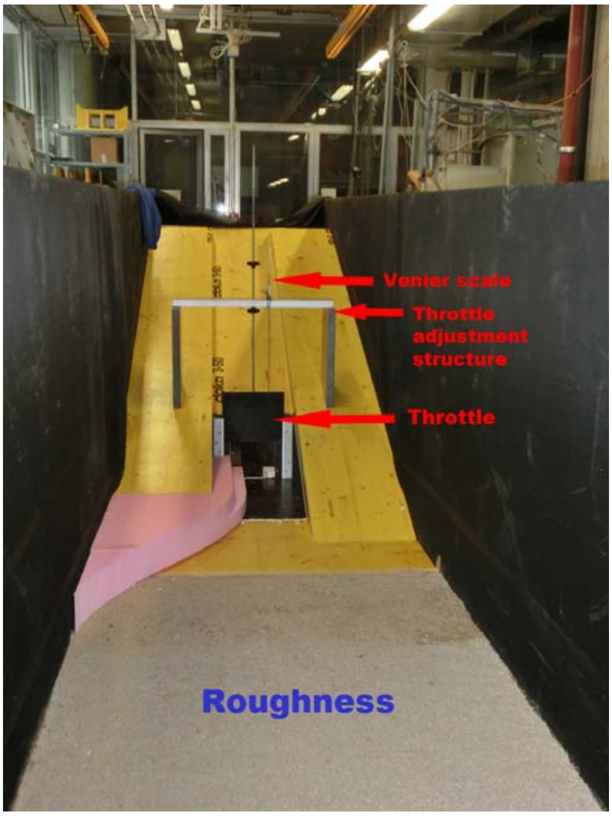

Figure 6: Upstream dam surface with adjustable throttle.

1.2.2.5 Water supply to the basin

At the upstream end of the retention basin an additional basin with a scum baffle was installed in order to get homogeneous inflow conditions over the width of the model (see Figure 7 and Figure 48).

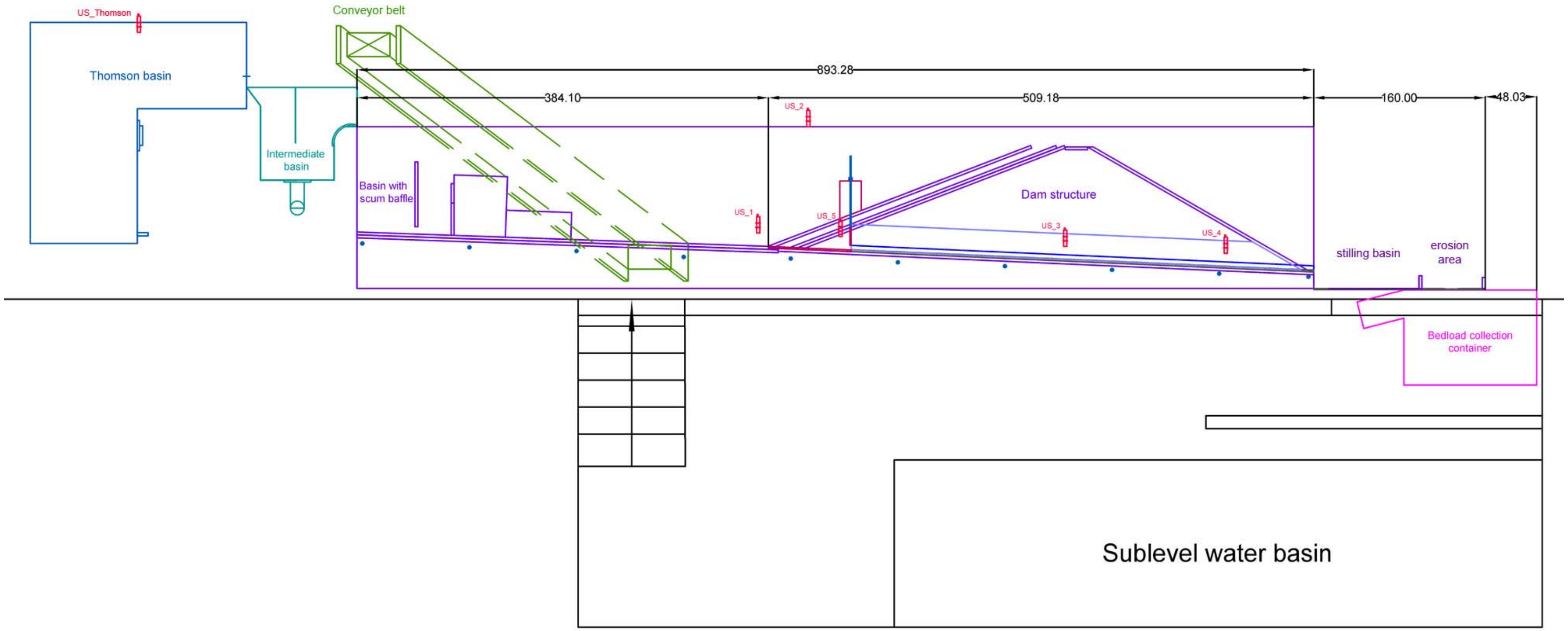

Figure 7: Longitudinal section plot model (dimensions in cm).

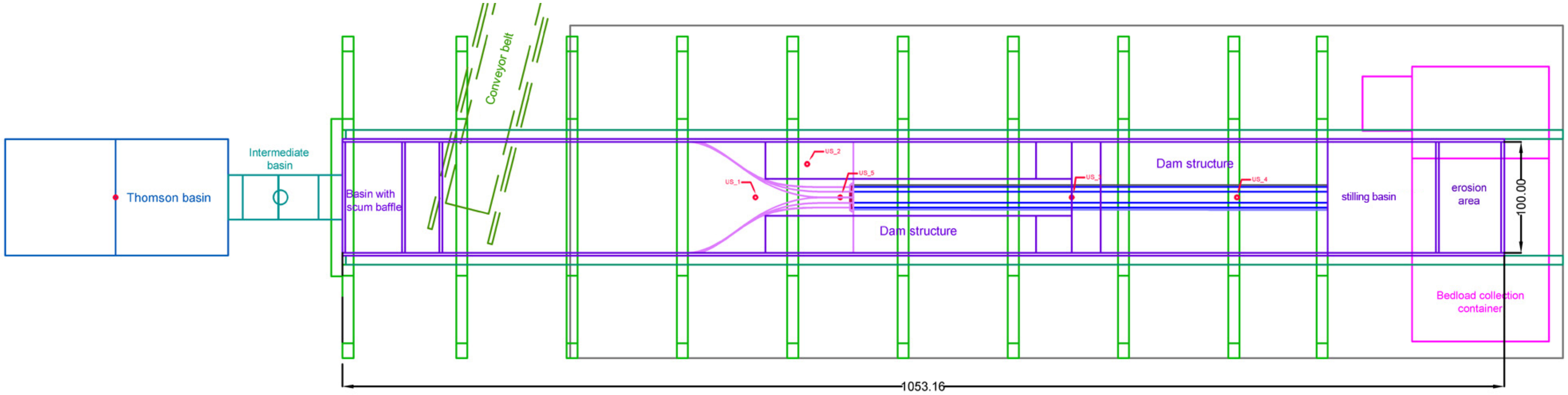

Figure 8: Plan view physical model (dimensions in cm).

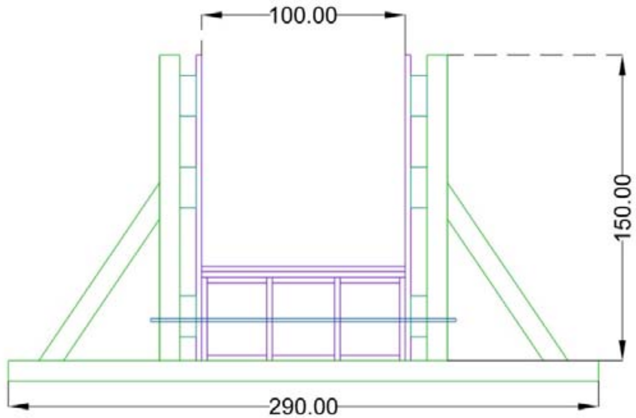

Figure 9: Section plot model (dimensions in cm).

1.2.3 Stilling basin and erosion area

A simple sealed wooden framework with a length of 1.6 m and a width of 1 m formed this section as a horizontal basin. A three-layer board separated the basin in two parts, so the dimensions of the stilling basin could be easily modified (see Figure 10). The height of the separation board followed the specifications of **alp**infra; the height of the board at the end of the model is based on the inclination of the culvert. During the period of the overflow investigation, the framework was adapted to assess this section in more detail.

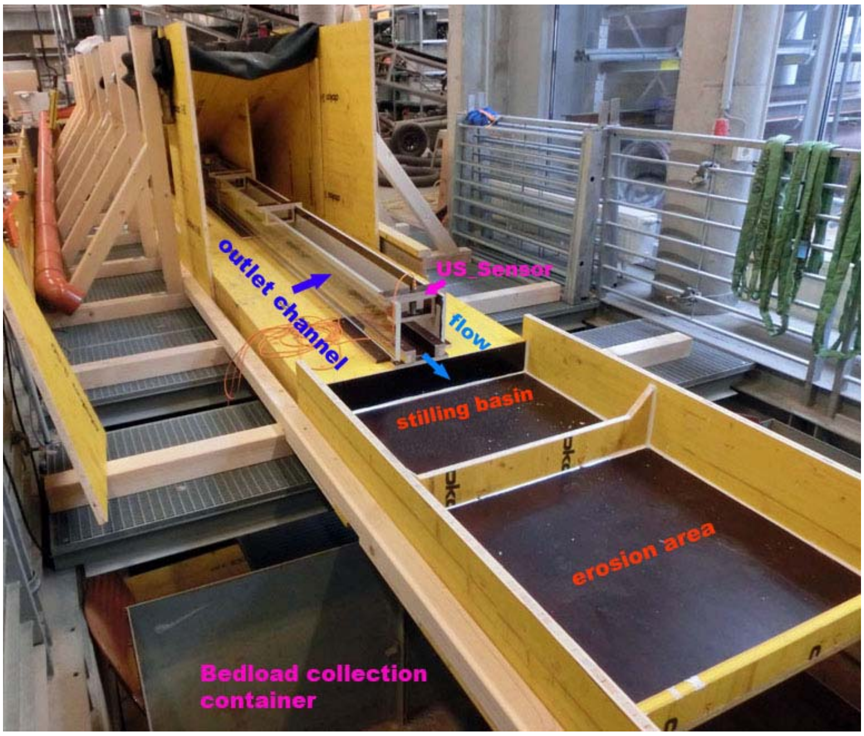

Figure 10: Stilling basin, erosion area and culvert structure.

Figure 11: Overview: physical sclae model base design.

Figure 11 shows the whole model including the conveyor belt in the back, the spillway the stilling basin and erosion area.

1.3 Sensors and measurements

1.3.1 Discharge

The pumping cycle of our laboratory includes a flowmeter between the circulation pump and the Thomson basin. This flowmeter (SIEMENS SITRANS F M MAGFLOW MAG 5000) informed about the actual discharge in l/s, and was controlled by the Thomson weir (see 1.3.3).

1.3.2 Water level heights

Figure 12 shows an ultrasonic sensor 'UC500-30GM-IUR2-V15' (PEPPERL + FUCHS GROUP, 2014).

Six ultrasonic sensors of this type were used during the tests. Sensor US_1 was placed in front of the rake, sensor US_5 directly upstream the throttle. Both were set close to the ground and when water was not retained, for tests with higher water levels these sensors were removed. Sensor US_2 gave information about the water level at filled up conditions. US_2 was installed on the left side when water was flowing and at the level of the left sidewall of the model (see Figure 13). Two other sensors (US_3, US_4) were placed in the tunnel, one at 2 m and the other at 3,5 m downstream the throttle.

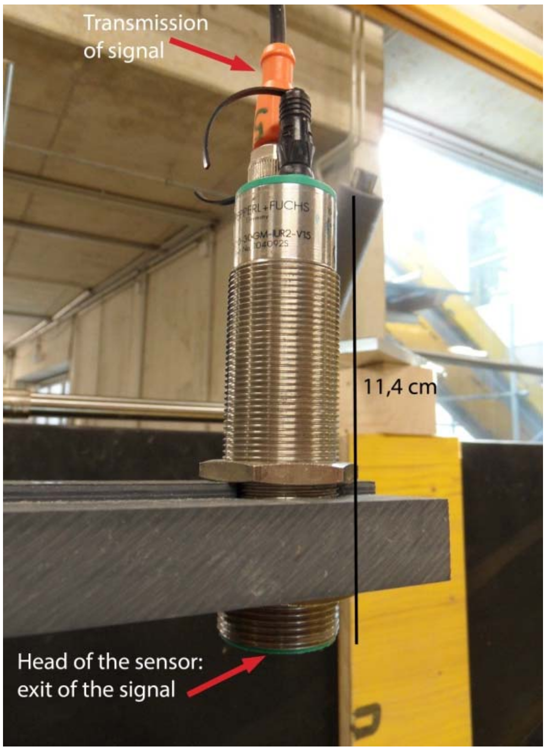

Figure 12: Ultrasonic sensor PEPPERL&FUCHS.

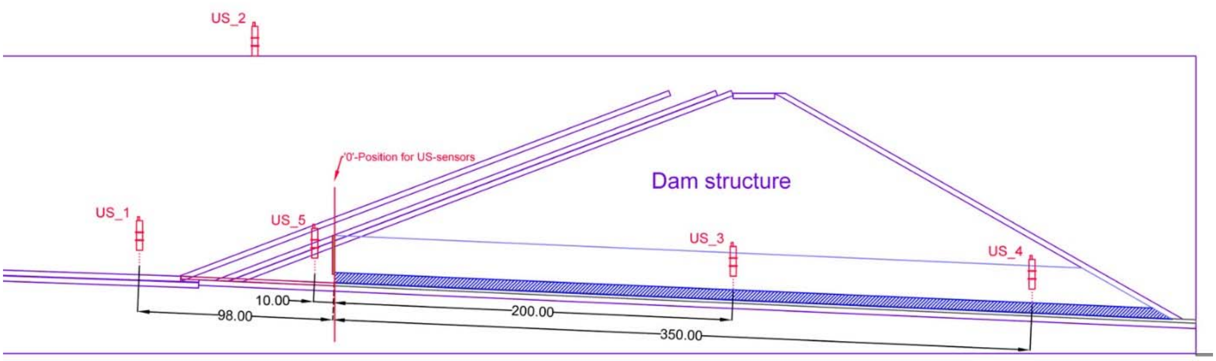

Figure 13: Positions of the ultrasonic sensors (dimensions in cm).

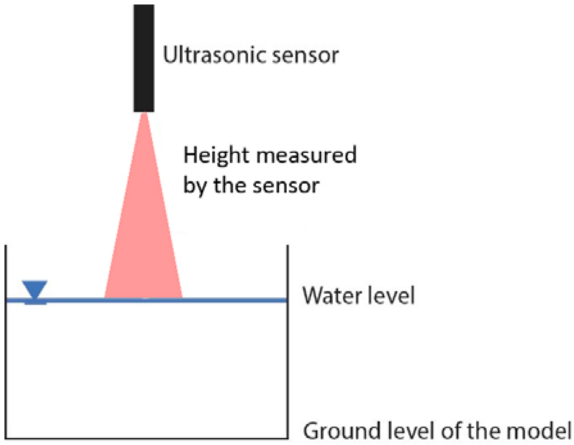

Figure 14: Drawing of the measured parameter with an ultrasonic sensor.

The sensors measure the distance between the base of the sensor and the water level (Figure 14). Knowing the distance between the fixed sensor and the ground level of the model, the water level can be determined. The ultrasonic sensors were operated with 10 Hz. The response of ultrasonic sensors is linear with distance and independent upon the reflectivity of water (ROCKWELL AUTOMATION Inc., 2015).

1.3.3 Thomson Weir

The sixth sensor (US_Thomson) was placed above the Thomson basin (see Figure 7). The outlet of this steel tank had a V-shaped profile with a specified angle. Combined with the US-sensor, which showed the water height, the accurate discharge was calculated to control the signal from the pump (see Figure 15).

According to PREIßLER and BOLLRICH (1985), this V-shape helps, to calculate the discharge:

$$Q = \frac{8}{15} * \mu * \sqrt{2g} * tan\alpha * h^{5/2}$$

With: $\mu = 0.565 + 0.0087/\sqrt{h}$

The parameters Q, g, h and μ correspond to:

Q, the discharge (m^3/s)

g, the gravitational acceleration (m/s^2)

h, the height of the water level (m)

μ, the discharge coefficient

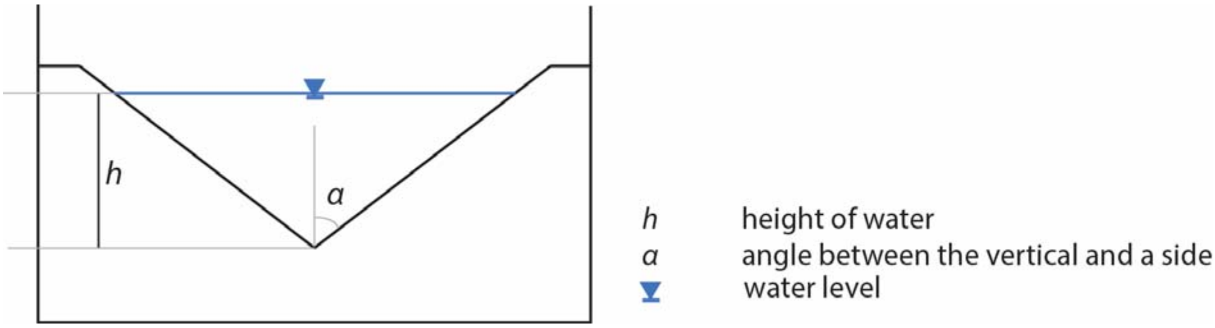

Figure 15: Drawing of the V-shaped Thomson basin (adapt. form PREIßLER and BOLLRICH, 1985).

1.3.4 Height of throttle opening

To measure the opening of the throttle at the inlet of the tunnel, a vernier scale was installed. One side was fixed to the top of the throttle and thus, the ruler was moving at the same time as the throttle (see Figure 16). The throttle opening is defined as the height between the bottom of the outlet channel and the bottom edge of the throttle.

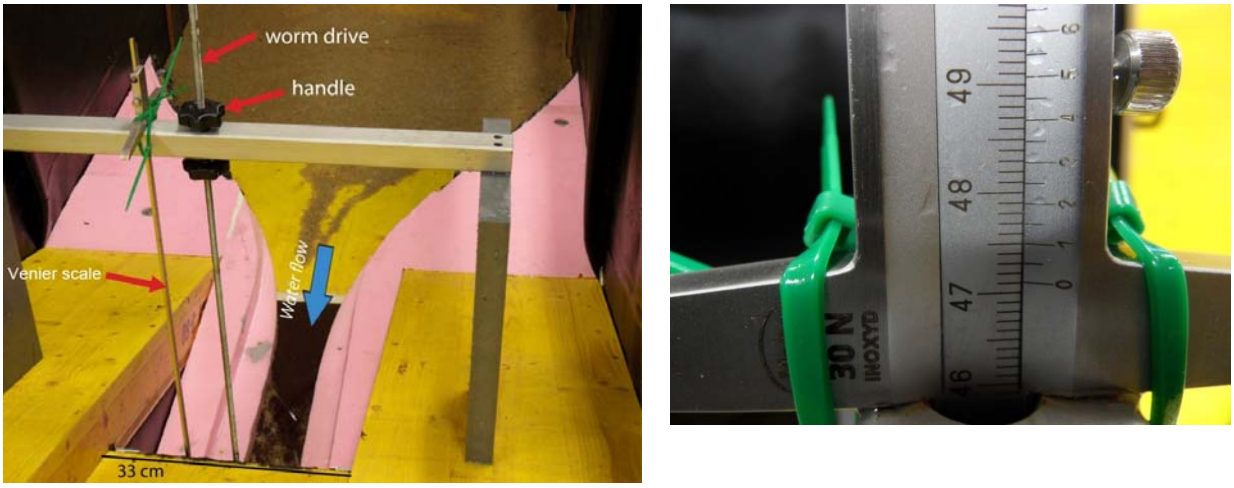

Figure 16: Vernier scale measuring the throttle opening height and detail of vernier scale.

1.3.5 Volume of the bedload deposition an remobilization

A two-step process generated the data for bedload deposition volumes in the retention basin.

1. In the first step the surface data was generated by using photogrammetry. For this purpose the Agisoft PhotoScan software was used. Eight targets were attached to the model and referenced to set dimensions in the lab (see Figure 48). During a bedload test run regular breaks were done to take photo series of the deposited bedload. The software

automatically detects the targets, and generates a 3D- model. For the next process the model was exported as TIFF file.

2. The ‘Surfer13’ (Golden Software) program was used to compute the deposition volumes of the 3D-models. Therefore it was possible to compare the volume data and visualize growth or re-mobilization of sediment.

1.3.6 Bedload transport capacity in the culvert

Sediment was transported through the culvert at different stages of the bedload tests. To get the information about the transport capacity, sediment was trapped at the downstream end of the culvert. A 0.5 mm (DIN 4188) sieve was taken to filter the material for a period of 1 minute per sample. The samples were dried and weighted, and an average value on the removal-time was calculated to get the unit kg/s.

1.3.7 Density of the bedload deposit

For density measurements of the sediment a sampling ring (inner diameter: 9.9 mm) was used. Sediment was sampled with the sampling ring at 3 positions in the retention basin: 1.2, 2 and 2.7 m upstream the throttle (Position ‘0’), in the middle of the basin. The samples were measured, dried and weighed.

1.3.8 Flow velocities

For recording the velocity distribution at the downstream face of the dam and in the outlet channel a flowmeter from Schiltknecht (MC20) was used. The small diameter of the impeller (1 cm inner diameter) helped to measure at small flow heights (Figure 17). The changed water surface height caused by entrapped air at the lower section of the dam, precluded flow velocity measurements based on ultrasonic sensors.

Figure 17: Flowmeter: Schiltknecht MC20.

1.4 Rakes

A central question for the physical modeling was to develop a rake structure that meets the following requirements.

- The rake should not affect the flow conditions at the throttle in a disadvantageous way.
- Woody debris should be trapped, to avoid blocking at the throttle and the outlet channel.
- Small bedload transporting events should pass almost undisturbed through the culvert but the rake should filter the coarsest fractions.
- The technical practicability on realistic conditions should be given, and the front should be modifiable for later adaptions.

Thus, different rakes were in discussion and tested during the experiments to meet the various issues. The designs of Rake#2 and Rake#2a were provided by **alp**infra, Rake#1, Rake#3 and Rak#4 were developed at the Institute of Mountain Risk Engineering.

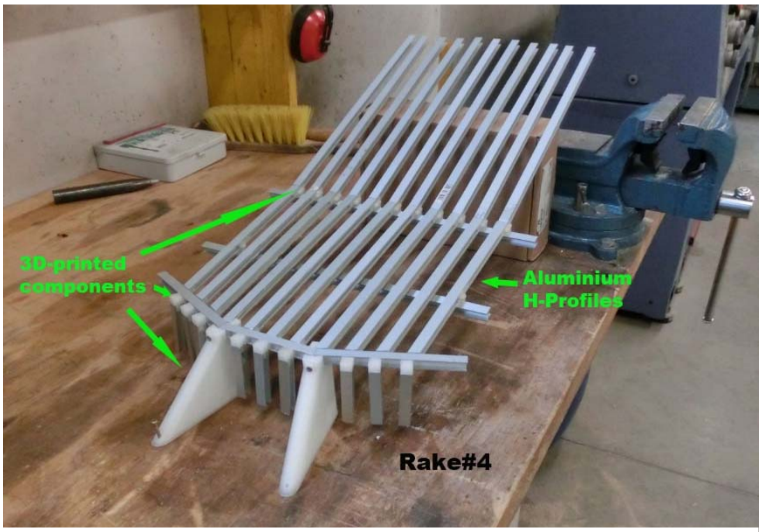

Figure 18: Model: Rake#4.

With the exception of Rake#1 the rake beams were made out of especially cropped 10 to 10 mm aluminum H-profiles. Other details and most of the required intersections were realized by 3D-printed components (see Figure 18). The vertical beams of Rake#1 showed a round cross section with a diameter of 10 mm, but on the upper side H-profile beams were placed.

1.4.1 Rake#1

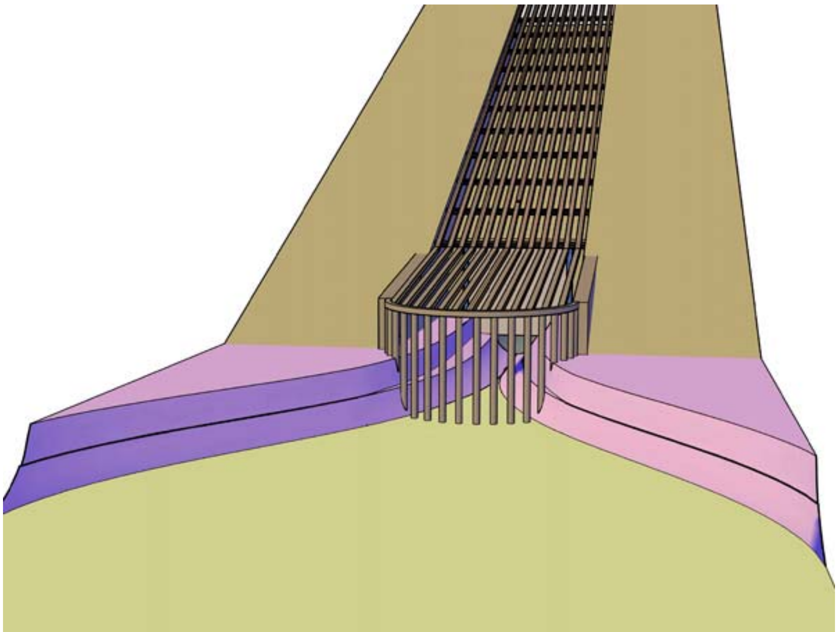

Figure 19: 3D-plot: Rake#1.

Like above-mentioned, the vertical beams of 'Rake#1' were made with round profiles. Also the upstream front of the rake showed a half circular section (see Figure 21) with a radius of 176.65 cm. The distance between the single beams was 2 cm. The upper beams showed a distance of 1.5 cm. On both sides of the rake additional (concrete)-flaps simplified the rake structure and guaranteed beneficial flow conditions at the throttle (see Figure 19). The hydraulic convenient vertical beams and the enlarged surface of the cross section should enhance high discharges without clogging.

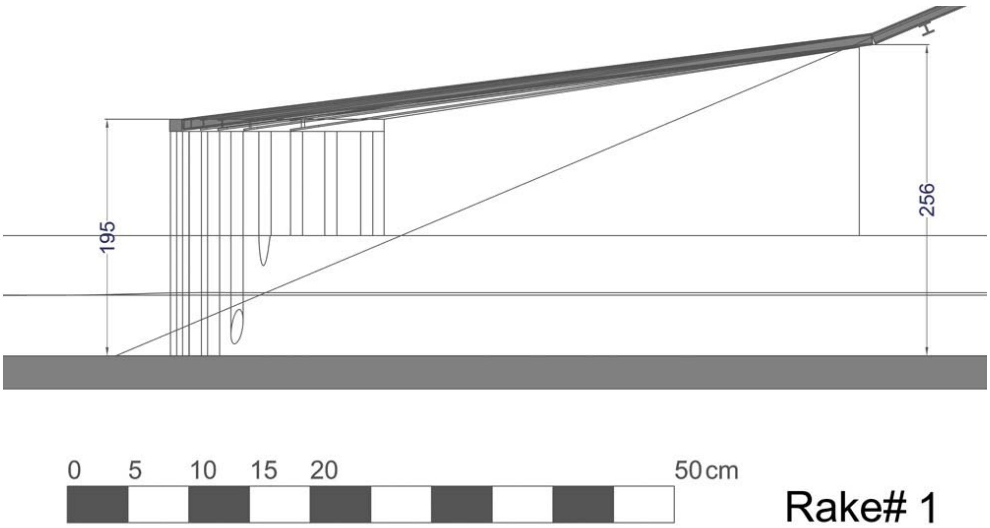

Figure 20: Longitudinal section: Rake#1 (dimensions in mm).

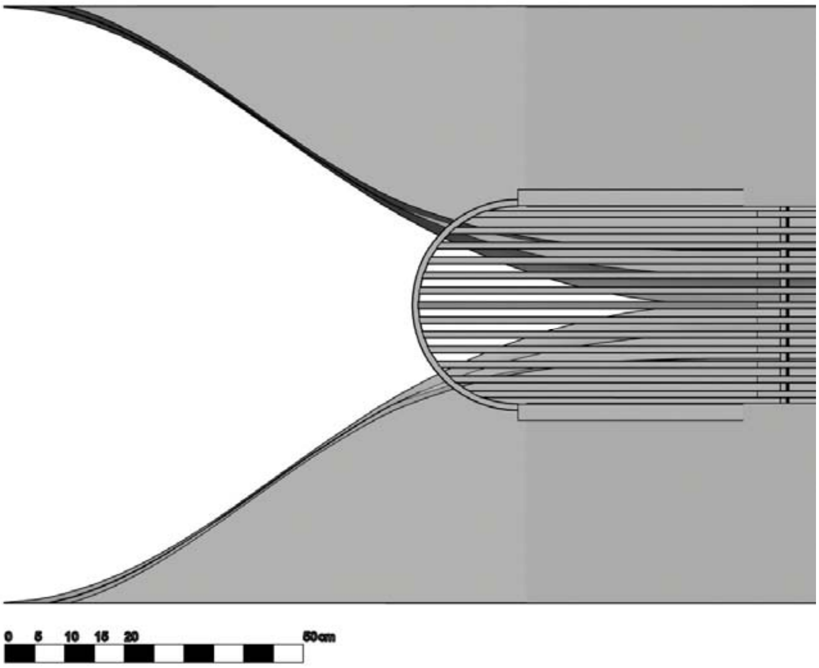

Figure 21: Plan view: Rake#1.

1.4.2 Rake#2

Rake#2 was designed as a simple rake following the inclination of the dam structure. The front section was built of vertical H-profile beams, which end 3.42 cm above the bottom. That distance correlated with the water height of 8 m^3/s discharge at this position. The distance between the beams was set to 1.5 cm (see Figure 22 to Figure 24).

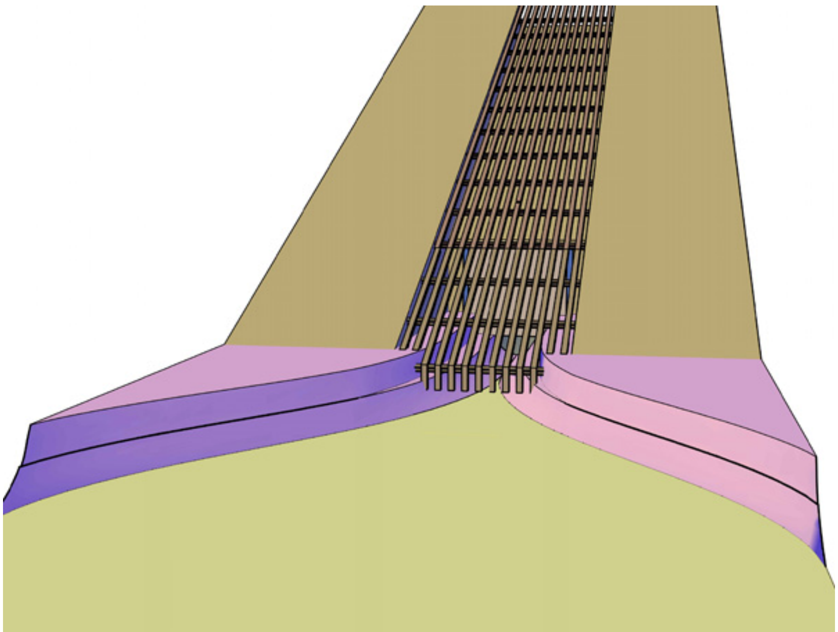

Figure 22: 3D-plot: Rake#2.

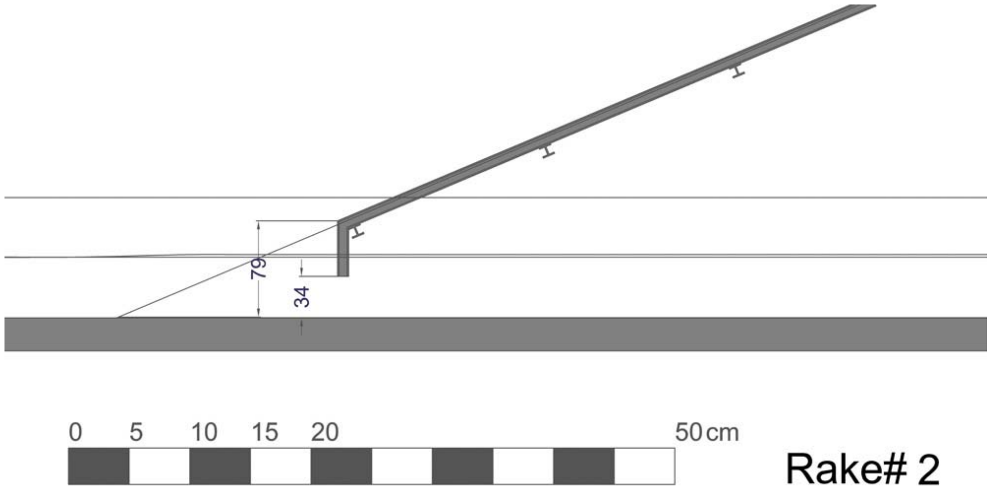

Figure 23: Longitudinal section: Rake#2 (dimensions in mm).

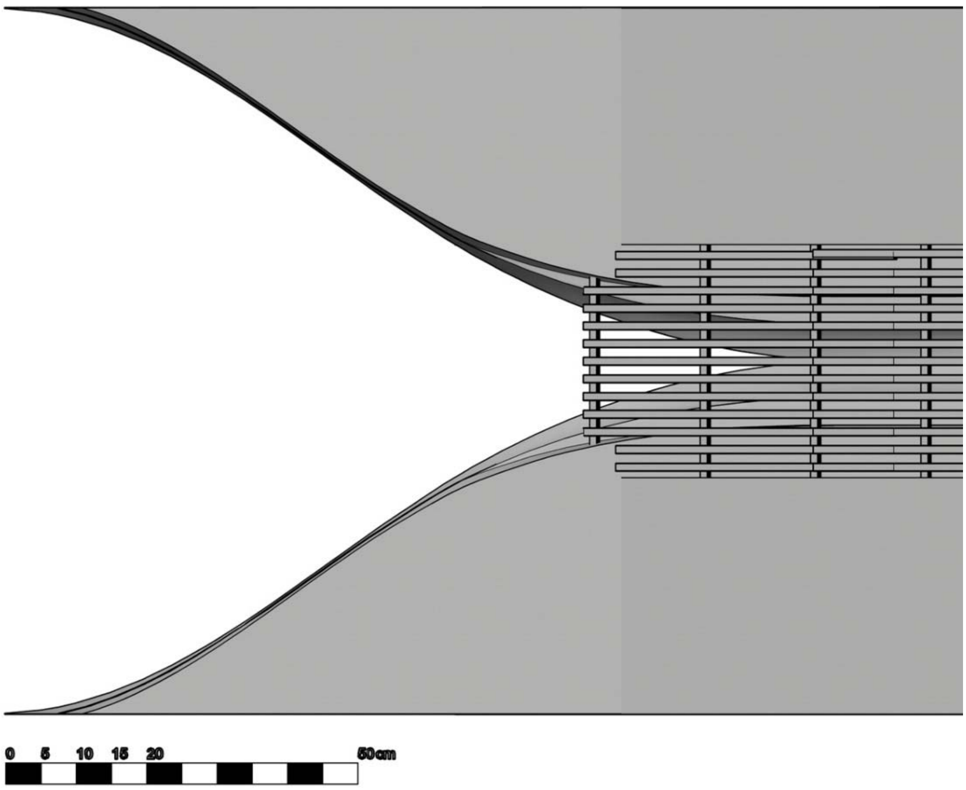

Figure 24: Plan view: Rake#2.

1.4.3 Rake#2a

The differences between rake#2 and rake#2a (Figure 25 to Figure 27) were in length and distance of the rake front to the ground. Therefore the rake was pushed forward to the position where the lower end of the rake met a distance to the bottom structure of 1.5 cm.

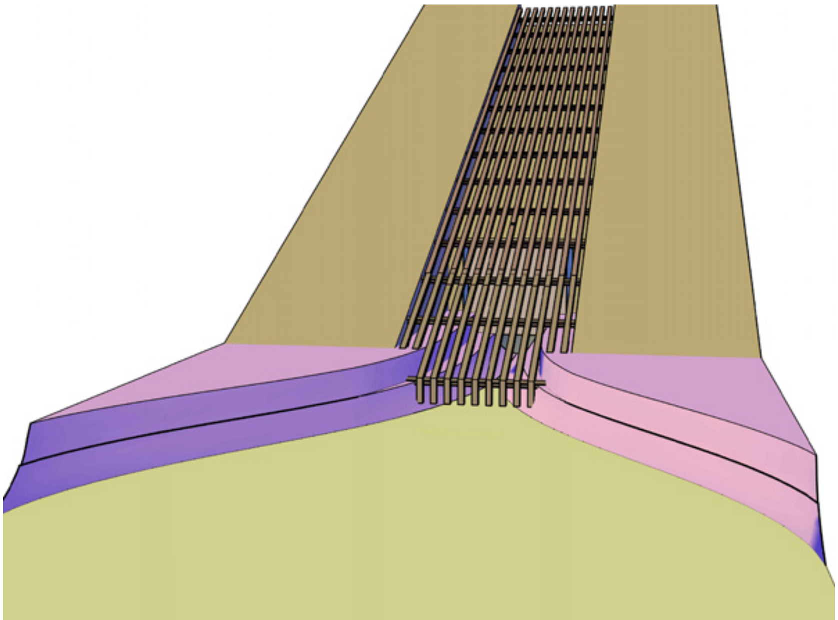

Figure 25: 3D-plot: Rake#2a.

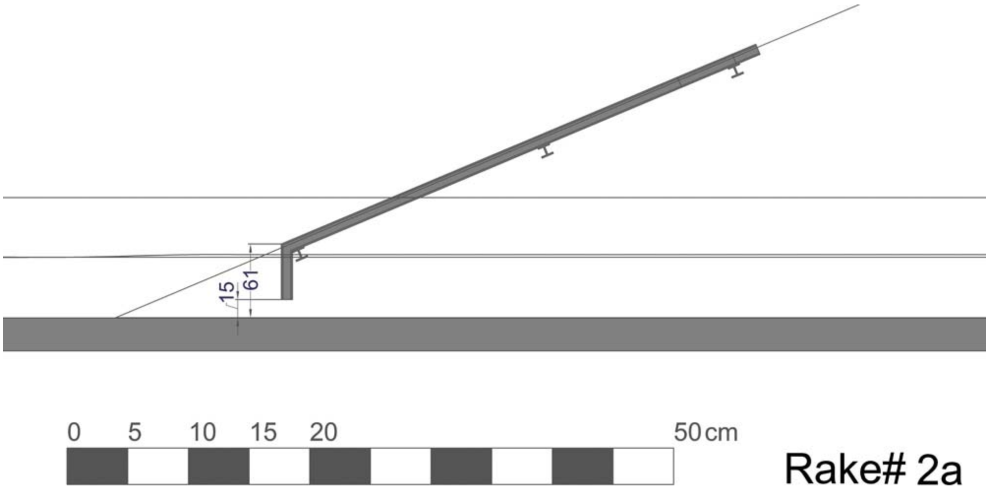

Figure 26: Longitudinal section: Rake#2a (dimensions in mm).

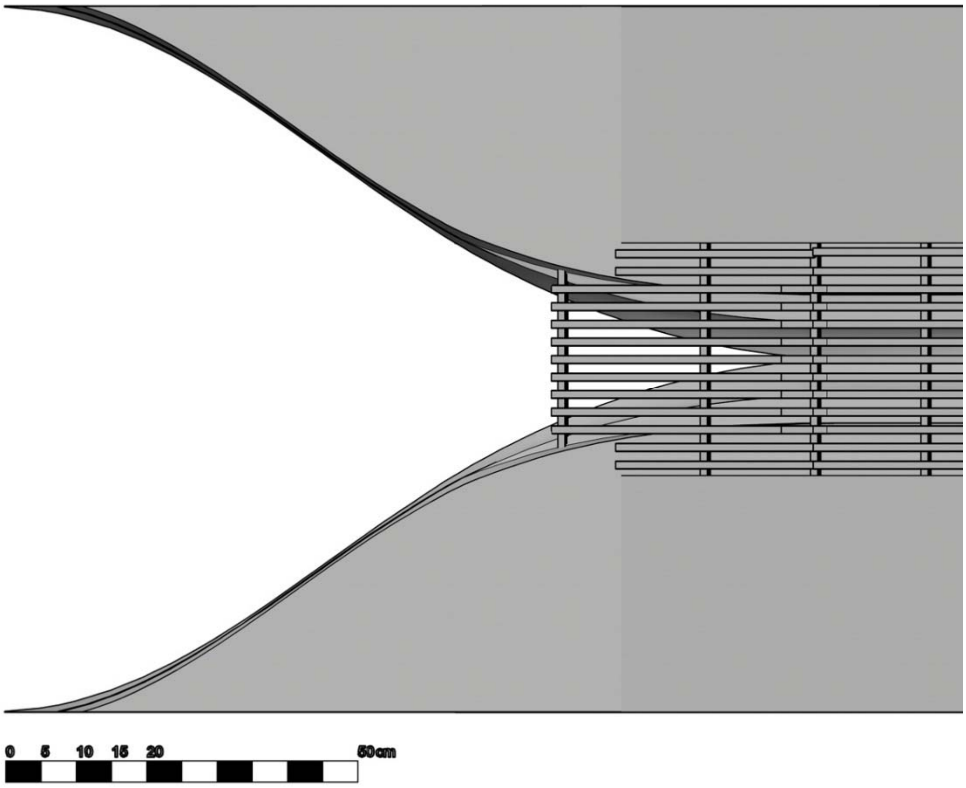

Figure 27: Plan view: Rake#2a.

1.4.4 Rake#3

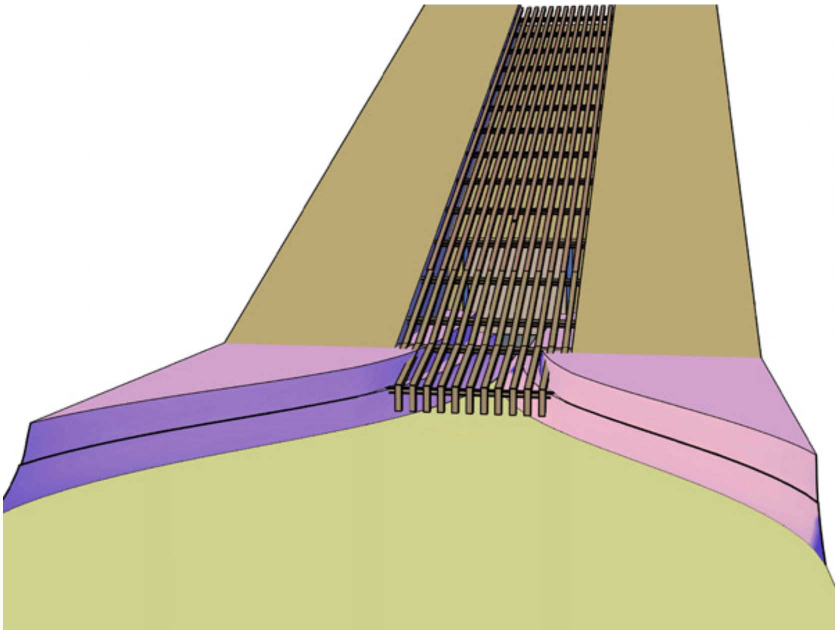

Figure 28: 3D-plot: Rake#3.

Rake type #3 showed two kinks, the upper one at a height of 9,7 cm over ground, the lower one at 6 cm (see Figure 28 to Figure 30). The beams on the front side ended 1,5cm above the ground. The inclination of the flatter middle section was 14°. The distance between the beams was again specified with 1.5 cm. That type was planned to filter out woody debris. The small height of the front beams forces the woody debris to deposit at the flat-angled area above and so avoid clogging in the lower parts.

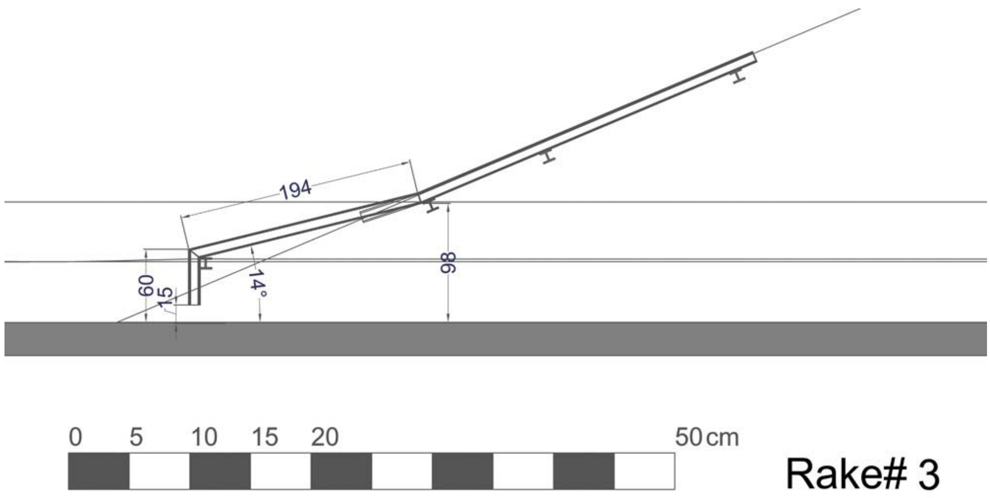

Figure 29: Longitudinal section: Rake#3 (dimensions in mm).

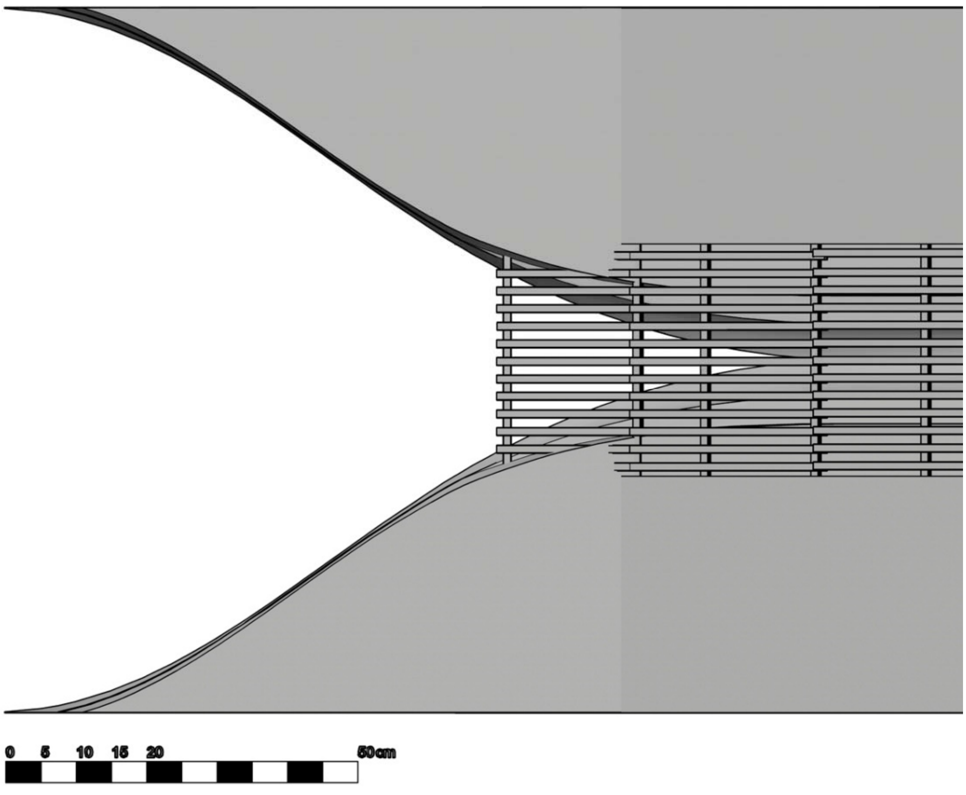

Figure 30: Plan view: Rake#3.

1.4.5 Rake#4

Rake#4 (Figure 31 to Figure 33) included two disks to support the rake and avoid clogging by woody debris. Additionally, the disks enhance water velocities at the rake and increase self-cleaning effects after sediment deposition. The disks were designed as triangles with a 45° angle, and a thickness of 1.67 cm (0.5 m nature scale). The upstream edges were constructed with round profiles; the length on the base was 11.67 cm (3.5 m nature scale).

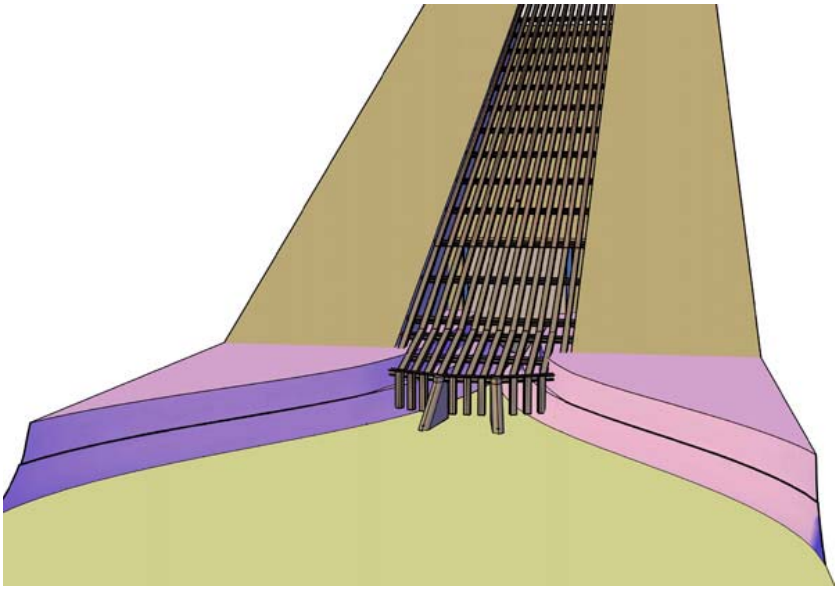

Figure 31: 3D-plot: Rake#4.

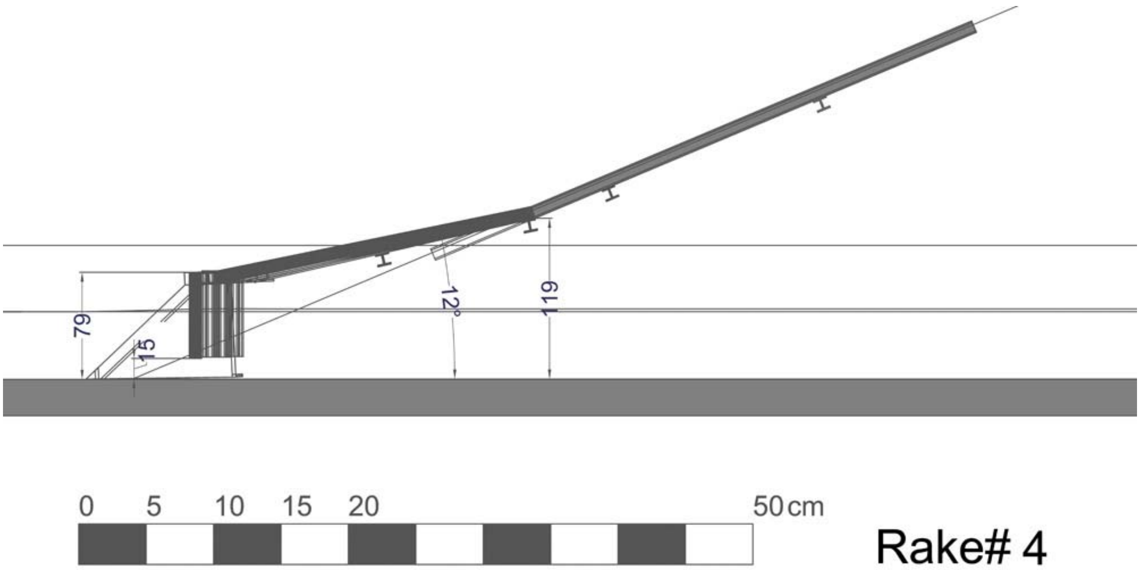

Figure 32: Longitudinal section: Rake#4 (dimensions in mm).

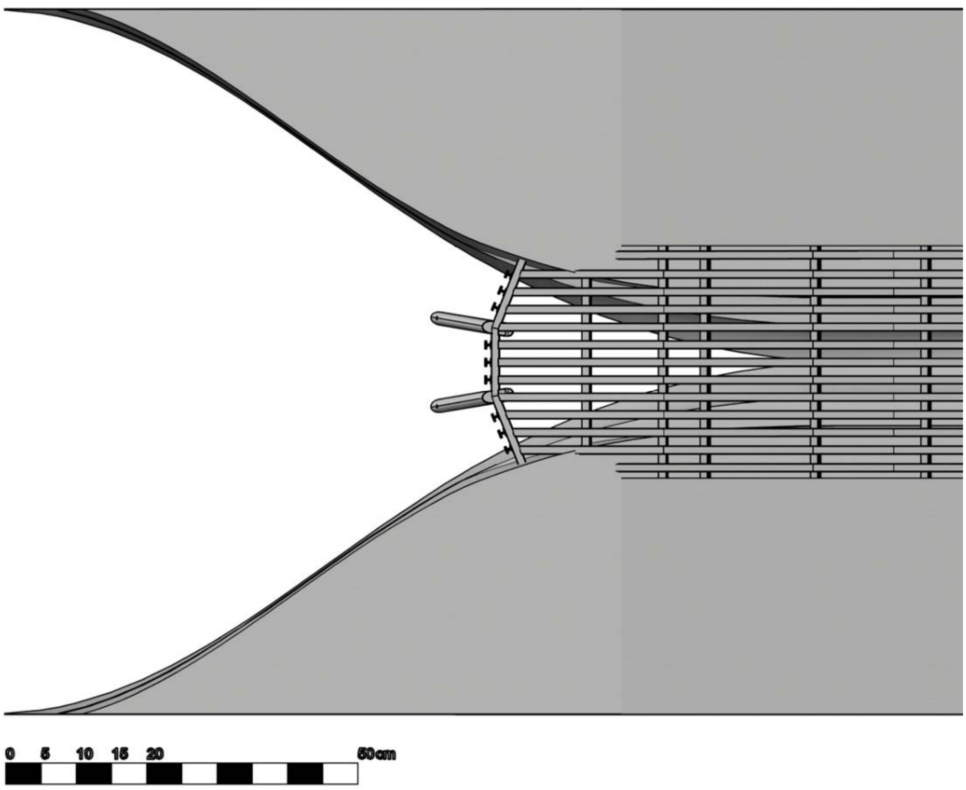

Figure 33: Plan view: Rake#4

2 Experiments

2.1 Hydraulic experiments

The hydraulic experiments should answer a series of issues around the outlet channel design, the inlet structure and throttle construction, as well as the rake structure. Four main test setups for the hydraulic experiments were determined to deliver sufficient results.

The hydraulic experiments were operated with steady state conditions. That means, a test needed to show constant values over a longer period of time. Only when steady conditions appeared, the measured values were used for evaluation. From the acquired values, a mean value was calculated which can be found in the result tables.

2.1.1 Types of the hydraulic experiments

2.1.1.1 Full basin (FB) test:

In a first step, the particular setup was run with the so-called 'full basin' or 'FB' test.

The retention basin was filled up with water to its top (see Figure 34). Then, the particular discharge was set to the water supply pump. Now, the throttle was adjusted to the asked maximal flows, so that the water height in the retention basin stayed constant over a specific period of time.

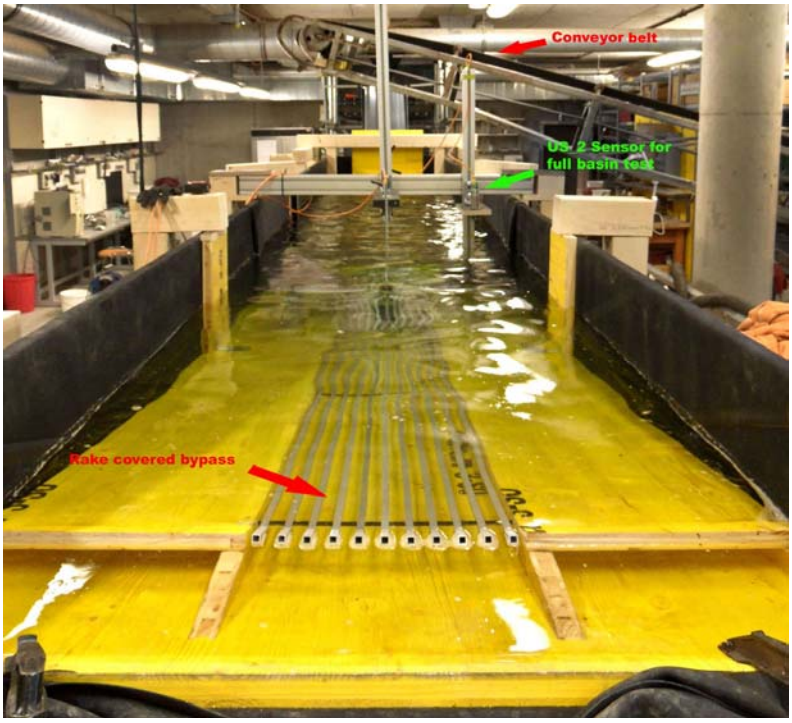

Figure 34: Retention basin at 'full basin' conditions.

2.1.1.2 Maximum discharge (MD) test:

In a second step, the maximum free surface flow without backwater effect at the determined throttle height was tested.

Therefore the throttle specifications from the 'FB' tests were used and the discharge gradually increased from '0' to the level where it showed the first backwater effects at the throttle (see Figure 35). This information was requested from the engineers, because the retention of water changes the flow conditions upstream the structure and for this reasons it also affects the bedload transport situation.

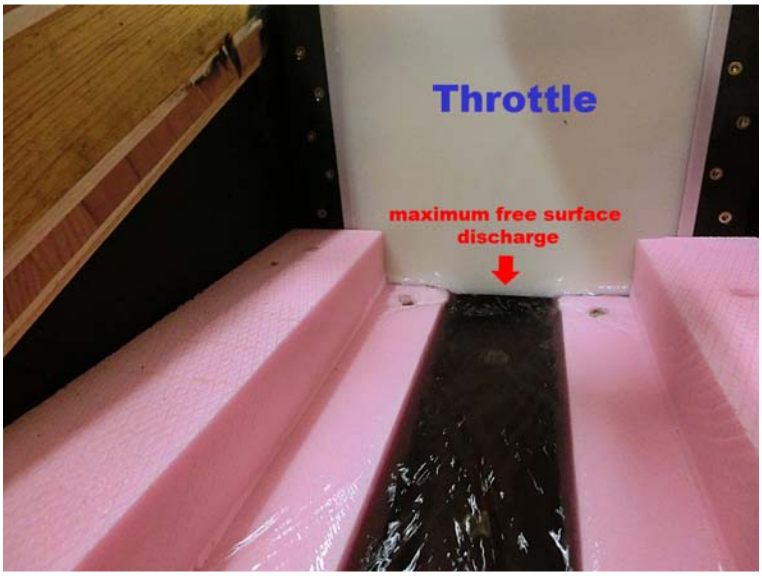

Figure 35: Throttle at maximum discharge conditions.

2.1.1.3 Normal flow (NF) test:

The 'NF-tests' focused on discharges below the 'maximum discharge'. Water heights on specified positions upstream the rake structure were measured, upstream the throttle and in the outlet channel. That setup provided information on the effects of different rake types and for the annual flows.

2.1.1.4 Overflow (OF) test:

For a possible overflow event, a 318 m^3/s scenario in natural scale was requested. The 318 m^3/s scenario (64.5 l/s in the model scale) would lead to an overtopping of the retention structure. As our model was limited to a width of 1 m and our pump to 50 l/s, it was needed to adapt the experiments. According to a proposal of **alp**infra, we built in a narrowing to 75.4 cm (22.6 m) width at the downstream face of the dam. Operated with a discharge of 48.7 l/s (240m^3/s) the setup matches the same height of the overflowing water at the dam crest. The 'OF'-experiments investigated the flow velocities along the downstream face of the dam, the flow conditions in the stilling basin, the bedload behavior in the stilling basin and the erosion area. Some additional installations (chute and baffle blocks) were tested. Apart from the velocity measurements, the effects were documented with pictures and videos.

2.1.1.5 Classification

For a better orientation a Test-ID system to number the single experiments was used. The code contains a series of numbers and letters describing the test setup.

- Pos1: **H -** (for 'hydraulics') test with only water; **BL** refers to 'Bedload'.
- Pos2: **E -** the outlet channel has a rectangular profile; R includes a round profile.
- Pos3: **OO -** for no rake; **Ra** for Rake#1; **Rb** for Rake#2; **Rc** for Rake#3; **Rd** for Rake#4; **Re** for Rake#2a.
- Pos4: **06, 08, 10, ... , 50, 60** or **100** for the value of the discharge tested (m^3/s),
- Pos5: **FB** for the simulation type 'full basin'; **MD** for the simulation type 'maximal discharge', **NF** for 'normal flow' tests.
- Pos6: **001** shows the sequence number of the test. If a test was repeated, the number rose.

Examples:

The file name **HE0050FB_001** means: it is a hydraulic test with the rectangular profile in the outlet channel, without rake and the type of simulation is 'full basin'. It is also the first test.

HRRd06NF_002: hydraulic test with the round outlet channel profile, rake#4 was installed, a discharge of $06m^3/s$ respectively 1.22l/s was used. It was a 'normal flow' test type and the second test with this setup.

2.1.2 Design of the outlet channel

In the progress of project planning, the cross section of the outlet channel was one of the first issues the physical modelling should deal with. The idea was to construct an outlet tunnel, which can be used for the discharge as well as for transport of deposited bedload material by trucks. Therefore the outlet channel had to provide a tunnel with appropriate dimensions of 5.5 m to 5.5 m for the trucks and an additional a discharge channel below.

Therefore, a squared U-profile basic structure with the maximum required dimension was installed (Figure 10). Later on, the channel profiles to test were installed. A throttle was fixed at the channel inlet, to reduce the cross sectional area according to the required discharge. For the tests, the throttle was adjustable in its height by a threaded rod, to find the adequate adjustment by testing (see Figure 6 or Figure 16).

2.1.2.1 Test with rectangular outlet channel

Following the specifications of **alp**infra, a rectangular channel cross section (see Figure 36) was tested with 45, 50, 60 and 100m^3/s. The goal was to find the particular throttle opening to achieve a maximum discharge of 45m^3/s under full storage condition. ('full basin': compare 2.1.1.1) In a second step the maximum free surface flow without a backwater effect for each throttle adjustment was tested. ('maximum discharge': compare 2.1.1.2)

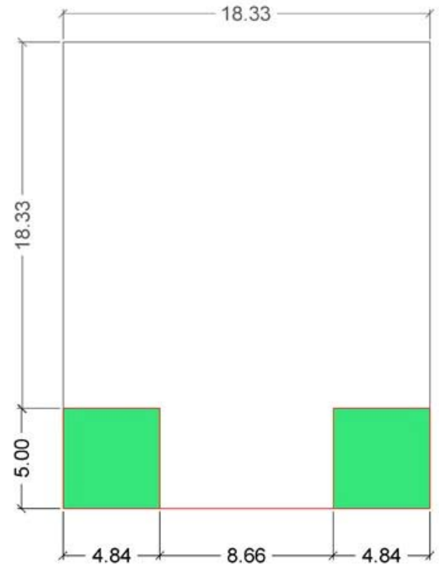

Figure 36: drawing of the outlet channel section (dimensions in cm).

In Table 2 the Froude conversion for the required discharges is shown.

Table 2: Froude-scaling the specified discharges.

Q real (m³/s)	Q model (l/s)
40	8.11
45	9.13
50	10.14
60	12.17
100	20.29

After running the 'full basin' and 'maximum discharge' experiments with the rectangular outlet channel, the results given in Table 3 can be shown. Figure 37 shows the corresponding throttle opening heights.

Table 3: Results of hydraulic experiments with rectangular outlet channel.

Rectangular outlet channel	Model condition			Real conditions		
	Discharge	Opening height: Throttle	Maximum discharge	Discharge	Opening height: Throttle	Maximum discharge
	l/s	cm	l/s	m³/s	m	m³/s
	9,13	3,83	2,80	45,00	1,15	13,80
	10,14	4,48	3,30	50,00	1,45	16,27
	12,17	5,49	3,90	60,00	1,65	19,23
	20,29	6,89	7,00	100,00	2,07	34,51

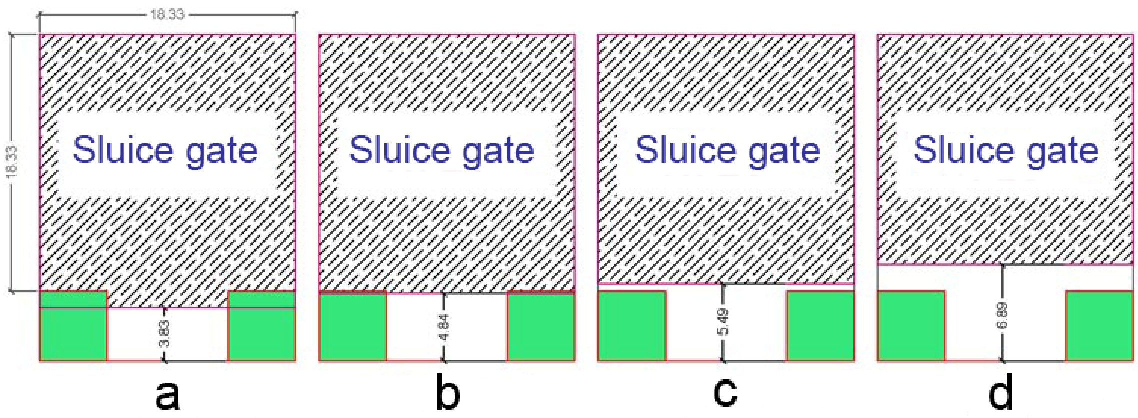

Figure 37: Different throttle opening heights (dimensions in cm).

Throttle opening height for 29 m pressure head at

a) 45 m^3/s
b) 50 m^3/s
c) 60 m^3/s
d) 100 m^3/s

2.1.2.2 Tests with round design of the outlet channel

The Institute of Mountain Risk Engineering suggested a round channel design for better sediment transport on lower discharges (see Figure 38). The Town of Canmore reduced the maximum discharge to 45 m^3/s. Thus, 'full basin' and 'maximal discharge' experiments were run with the specified maximum discharge only. A roughness corresponding to a steel surface was chosen for these investigations to protect the original outlet channel profile from abrasion by bedload transport. Furthermore, the smooth surface prevents sediment deposition.

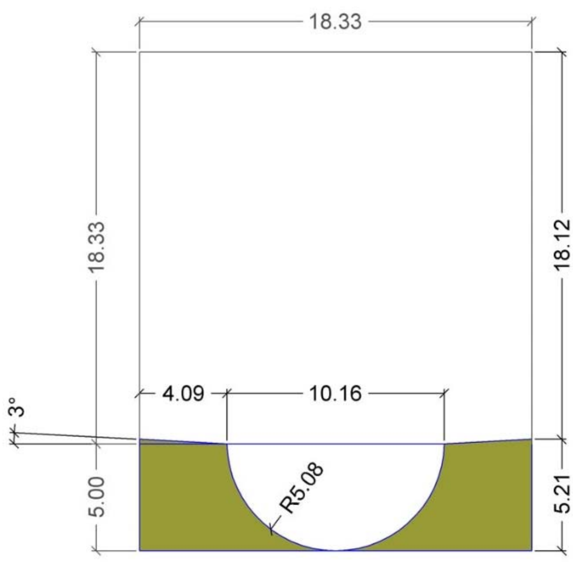

Figure 38: Round channel cross section (dimensions in cm)

For the 'full basin' tests a water head of 29.85 m (in real scale) at the lower edge of the throttle was asked by **alp**infra. For this water head the experiment determined a throttle opening height of 4.34cm - 1.3m in real dimensions. The ‘maximum discharge’ test showed a discharge of 2.75 l/s, which means 13.6 m^3/s for real conditions.

The following experiments were all run with the round design of the outlet channel.

2.1.3 Effect of throttle design

In a next step, effects of different throttle designs should be shown. To this end, two types of throttles were compared, in which the main design was the same, but the lower edge shape changed (see Figure 39). The test-ID with the additional ‘a’ in Table 4, shows the experiments with the 45° angle shaped throttle.

As it can be seen in Table 4, the throttle opening height varied 0.5 mm and led to a difference of 3.4 mm of the water height in the retention basin. Considering the accuracy of the single measurements and the period of several hours to get stable conditions the presented deviations are negligible. It has to be mentioned, that a hydraulically optimized design would lead to an outlet with a smaller opening height. In order to maximize the ‘maximum discharge’ that does not result in backwater effects, a hydraulic unfavorable design is preferable. This is the reason why no other designs like tainter gates or rolling gates were tested.

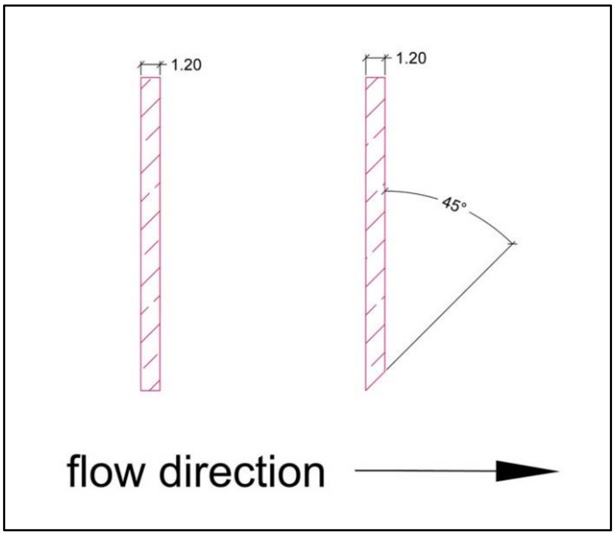

Figure 39: Compared throttle designs (dimensions in cm).

Table 4: Effects of 2 tested throttle designs.

	US_2	Pump	Throttle opening height	Square area
	[mm]	[l/s]	[cm]	[cm²]
HR0045MD_001		2,76	4,34	33,04
HR0045MDa_001		2,75	4,39	33,55
HR0045FB_001	969,29	9,14	4,34	33,04
HR0045FBa_001	965,88	9,14	4,39	33,55

2.1.4 Effect of rake designs

The model runs showed that with a filled basin the different rake types have no effect on the flow. Thus, we focused on tests at 'normal flow' (compare: 2.1.1.3) conditions to observe the influences of different rakes. The discharge was set in steps of 2 m^3/s in nature, from 6 to 14 m^3/s (see Table 5).

Table 5: Conversion after Froude: Nature to model.

Nature	**Model**
m^3/s	**l/s**
6,00	1,22
8,00	1,62
10,00	2,03
12,00	2,43
14,00	2,84

The height of the flow was measured at 3 Positions:

- Upstream of the rake structure (pos: -98). Depending on the particular rake, the distance between rake structure and measurement changes.
- 10 cm upstream the throttle (pos: -10).
- In the outlet channel, 200 cm downstream the throttle (pos: 200).

This setup specified the hydraulic properties for the 5 tested rake types. Figure 40 shows a comparison of all rake types at different discharges.

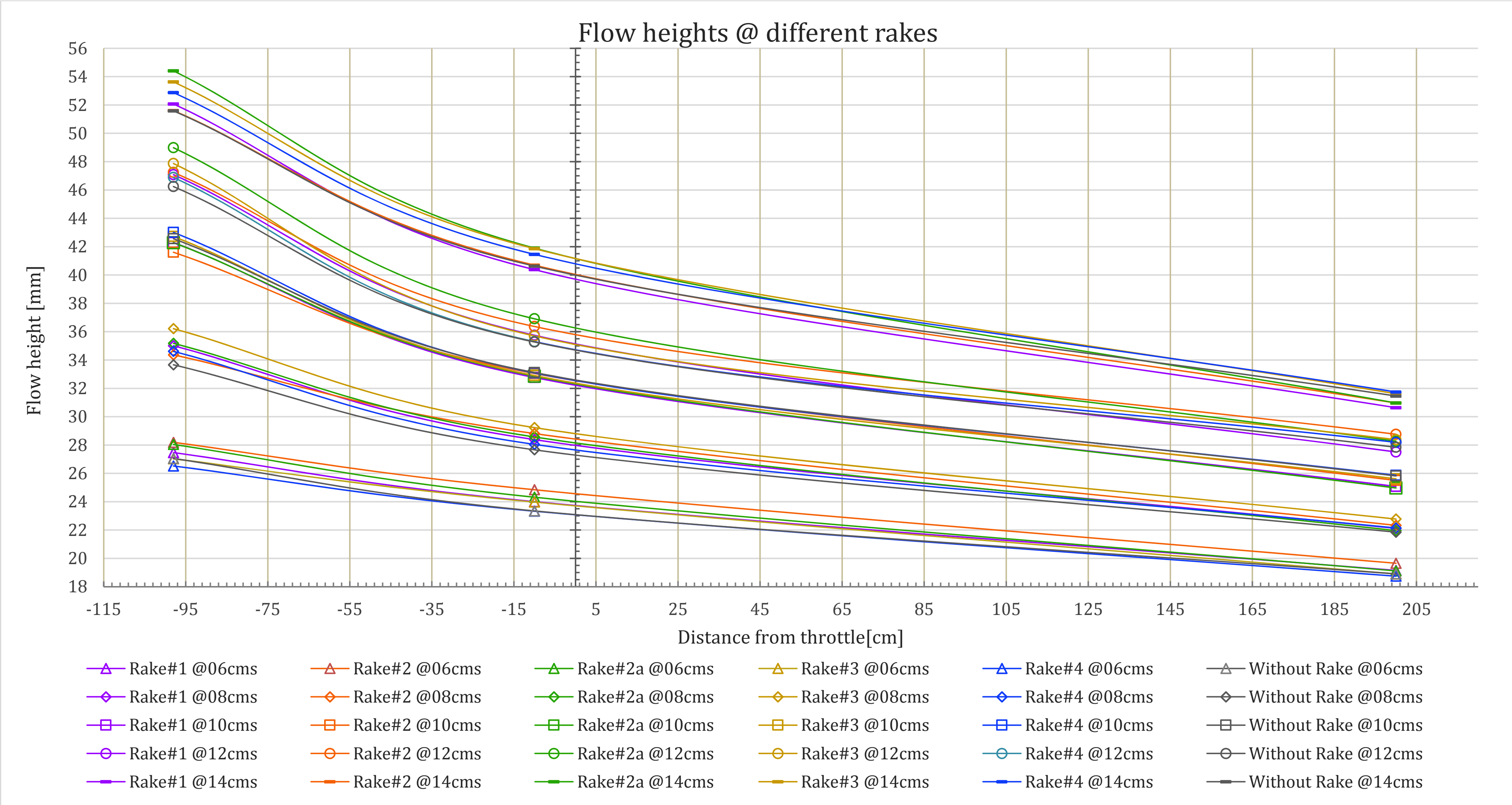

Figure 40: Heights of the flow at 3 positions along the model. The '0'-Line shows the position of the throttle. Position '-98' is just upstream the rake structure, position '200' displays the data from the US-sensor in the outlet channel.

The highest deviations can be found in the values at position '-98' upstream the rakes (Table 6). These are caused by the particular construction reducing the discharge section. Rake#2a and Rake#3 showed the biggest backwater effects at discharges corresponding to 12 and 14 m^3/s. These were also the ones to have horizontally installed beams on the lowest level (cf. 1.4). At position '-10' and '200', the deviations show values below 1.7 mm, which is within the accuracy of our measurements.

Table 6: Maximum deviation of the water height between different rakes at particular discharges (values in mm).

Discharge	Position to throttle		
	-98,00	-10,00	200,00
06 m^3/s	1,67	1,51	0,91
08 m^3/s	2,55	1,56	0,70
10 m^3/s	1,40	0,35	0,90
12 m^3/s	2,74	1,64	1,25
14 m^3/s	2,83	1,52	1,11

2.1.5 Effect of the inlet design and positioning of the rake

Even if the rake structure has a little impact on the flow conditions, the shape of the inlet and the distance between rake and throttle do. This impact was observed on conditions without retention of water at the throttle, up to 13.6 m^3/s in real scale, respectively.

In our set up the outlet channel was extended 30 cm upstream as a parallel channel, before it opened up towards the basin. The funnel leading into the parallel channel was hydraulically optimized (see Figure 8 or Figure 19 to Figure 33) to guide the water to the throttle.

The greatest backwater effects were observed in the last part of the funnel, just upstream of the starting point of the parallel channel profile. The parallel profile resulted in an increased flow velocity. A higher velocity means lower flow depth (see Figure 41). So, the maximum discharge can be increased by optimizing the area of acceleration, upstream the throttle.

If the rake structure - independent from the design - was installed too close to the area of flow acceleration, first backwater effects at the throttle could be observed at smaller discharges.

For the case of an empty basin a hydraulic jump was observed upstream the rake. Depending on the discharge it was observed at locations between about 205 cm (at 14 m^3/s) and 150 cm (at 6m^3/s) upstream the throttle. With a partially sediment filled retention basin these effects were not observable anymore due to the increased roughness of the deposited bedload material.

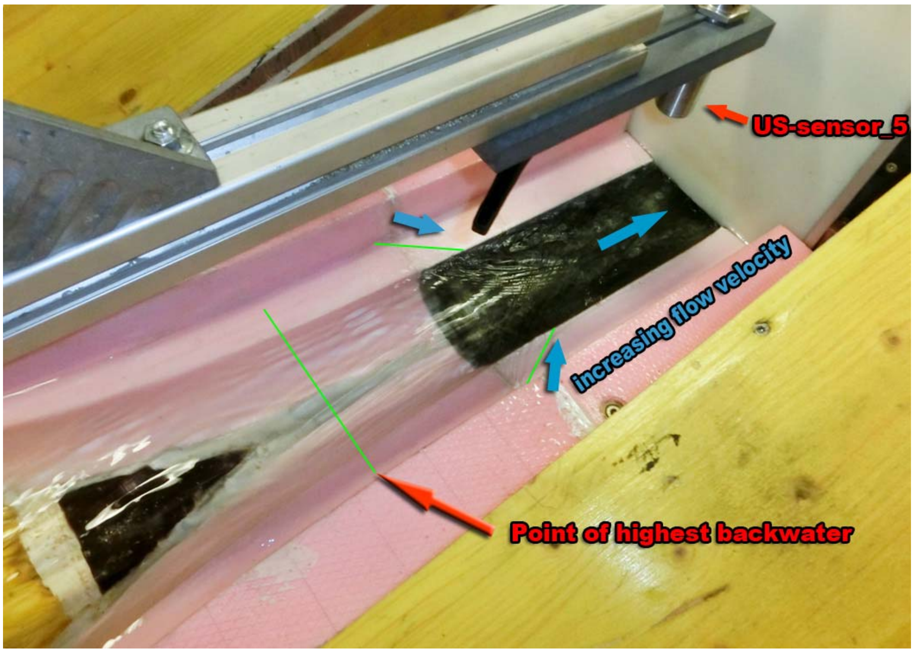

Figure 41: Inlet design upstream the throttle.

2.1.6 Length of the overfall

Figure 42 shows a sketch of the nappe at the channel outlet. The distances (values in natural scale) were measured at the intersection of the upper and lower nappe and a horizontal line at the height of the downstream boundary wall crest of the stilling basin. The measurements were done on 'full basin' conditions. The velocity shown in Figure 42, was calculated by the water height in the outlet channel (US_4 showed 1.23 m water height, diameter of the outlet channel 3,05 m) and the discharge (45 m^3/s), and it was measured by a flowmeter as well (see 1.3.8).

Calculation for the velocity:

$$v = \frac{Q}{A}$$

The parameters v, Q and A correspond to:

v, velocity (m/s)

Q, discharge (m^3/s)

A, flow area (m^2)

The calculated and measured velocity was scaled following the scale ratio after Froude (see 1.1).

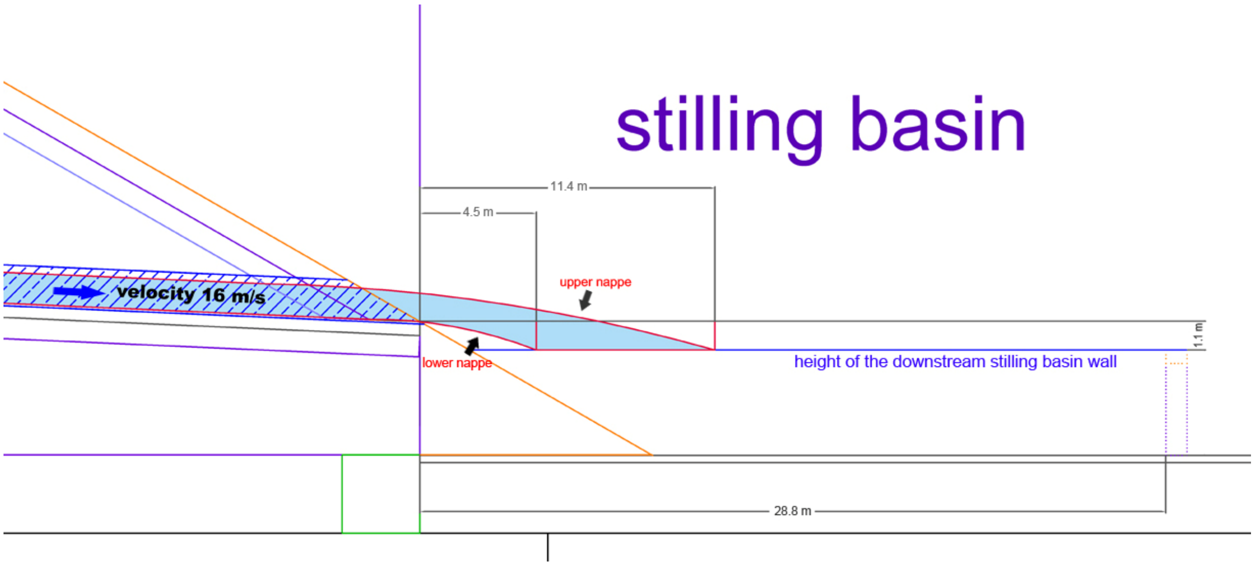

Figure 42: Sketch of the longitudinal section of the nappe at 'full basin' conditions.

2.1.7 Discharges at different storage levels

Figure 43 shows the correlation between a given discharge and the water level in the retention basin. The opening height at the throttle was 1.3 m in natural scale. The measurements were made 3 m (10 cm in model scale) upstream of the throttle (position of the sensor US_5), so that backwater did not affect the measurements. The given values represent the water surface height at the throttle, measured from the outlet channel bottom. The data were recorded at steady state conditions.

A transition from free flow to pressure flow occurs at 13.6 m3/s in natural scale. However, this flow rate can occur as either free flow or pressure flow under different circumstances.

With rising stage the water height for a rate of 13.6 m3/s is about 1.3 m (natural scale) under free flow conditions. The free flow continues until the flow rate exceeds 13.6 m3/s or if the flow is disturbed by, e.g. a tree reaching the rake. In the latter case backwater effects occur and the storage level reaches a height of 4 m (with a steady flow of 13.6 m3/s). Only if the flow level drops below this rate, the storage level decreases.

If the basin is filled and the inflow decreases to 13.6 m3/s the storage height remains 4 m until the flow continues to drop.

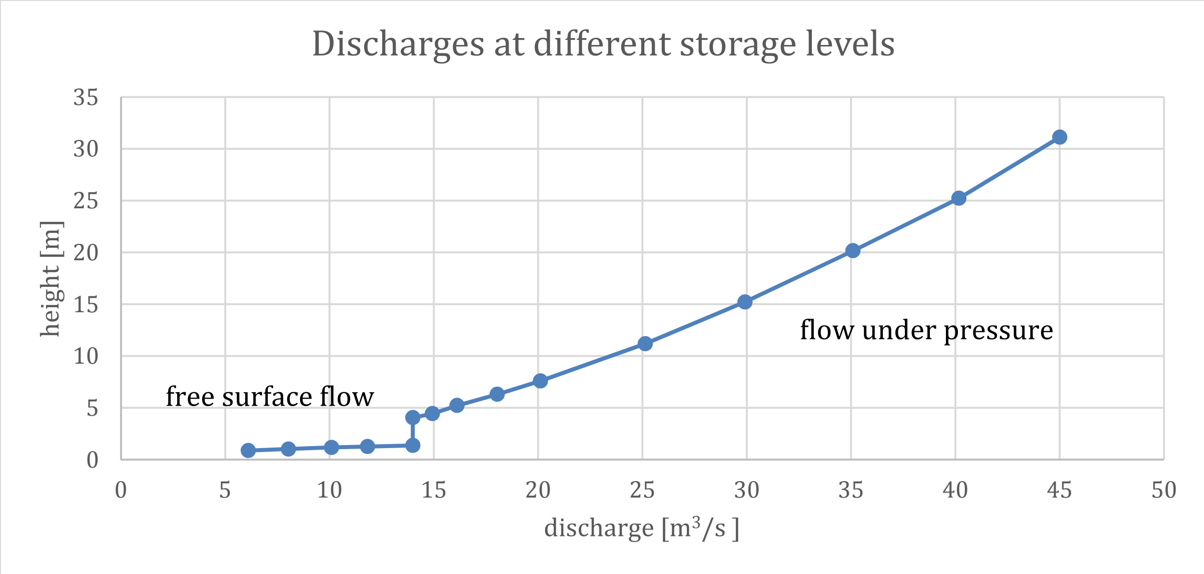

Figure 43: Water surface heights at different discharges.

2.2 Experiments with woody debris

Tests to observe the effects of the different rake designs were performed in order to analyze their ability of retaining woody debris. 4 types of rakes were used for this test batch (Rake#1, Rake#2a, Rake#3, Rake#4). Rake#2 was excluded, because of its high permeability, due to the high basal outlet design.

2.2.1 Test setup

A discharge of 2.43 l/s (12 m^3/s in natural scale) guaranteed a maximum of woody debris transport, without backwater effects. The throttle opening with 4.34 cm in the model remained equal to the maximum discharge conditions downstream the dam.

Round beech wood sticks with a length of 140 mm was used to simulate woody debris. The sticks were split up in three different diameters: 6 mm ('S' for small), 11 mm ('M' for medium) and 15 mm ('L' for large). According to the low level flow conditions upstream of the rakes, the woody debris was supplied 110 cm upstream the throttle ('0'-position see Figure 13) in the middle of the channel. For a test scenario 4 bundles of sticks were used, including 4S, 4M and 2L. For a random distribution of the wood sticks over the whole width of the channel a bundle of sticks was released at 40 cm height, stick by stick in a vertical orientation. Therefore a specified order (M-S-L-M-S-M-S-M-S-L) in a sequence of about one second was used. During one test, 4 bundles in a sequence of about one minute were brought in. Besides the number and type of the sticks passing the installed rake was recorded. For each rake the test was repeated 5 times.

Dry beech wood has a similar density as green spruce. Therefore, the sticks were dried between the single test-runs. Table 7 shows the mean number of sticks and the related standard deviation that passed the rake for the above-described setup (average of 5 tests per rake).

Table 7: Mean number of wood pieces that passed the rake.

Woody Debris		S	M	L	Sum SML
Rake#1	Mean	1.2	2.6	1	**4.8**
	Stan. Dev.	2.17	2.30	1.00	**4.55**
Rake#2a	Mean	2	1.4	0	**3.4**
	Stan. Dev.	2.35	1.67	0.00	**3.85**
Rake#3	Mean	0.8	0.8	0	**1.6**
	Stan. Dev.	0.84	1.10	0.00	**1.82**
Rake#4	Mean	0.4	0.6	0	**1**
	Stan. Dev.	0.55	0.55	0.00	**0.71**

All woody debris that passed the rake was transported through the outlet channel without deposition in the outlet channel or clocking of the throttle.

2.2.1.1 Rake#1

On average 4.8 sticks out of 40 passed rake#1. It is the only rake type, were wood of the category L passed. A typical pattern of how the wood is retained in front of the rake is shown in Figure 44.

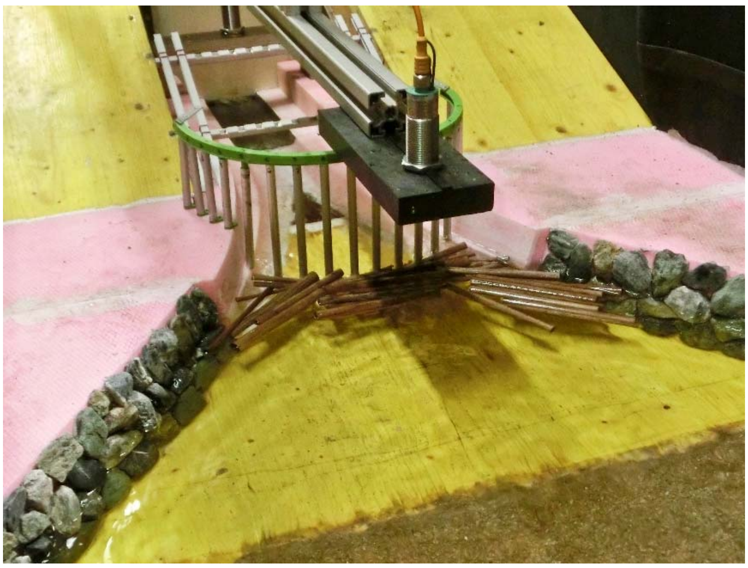

.

Figure 44: Woody debris in front of rake#1.

2.2.1.1 Rake#2a

On average 3.4 sticks out of 40 passed rake#2a. A typical pattern of how the wood is retained in front of the rake is shown in Figure 45.

Figure 45: Woody debris in front of rake#2a.

2.2.1.2 Rake#3

On average 1.6 sticks out of 40 passed rake#3. A typical pattern of how the wood is retained in front of the rake is shown in Figure 46.

Figure 46: Woody debris in front of rake#3.

2.2.1.3 Rake#4

On average only 1.0 stick out of 40 passed rake#4. A typical pattern of how the wood is retained in front of the rake is shown in Figure 47.

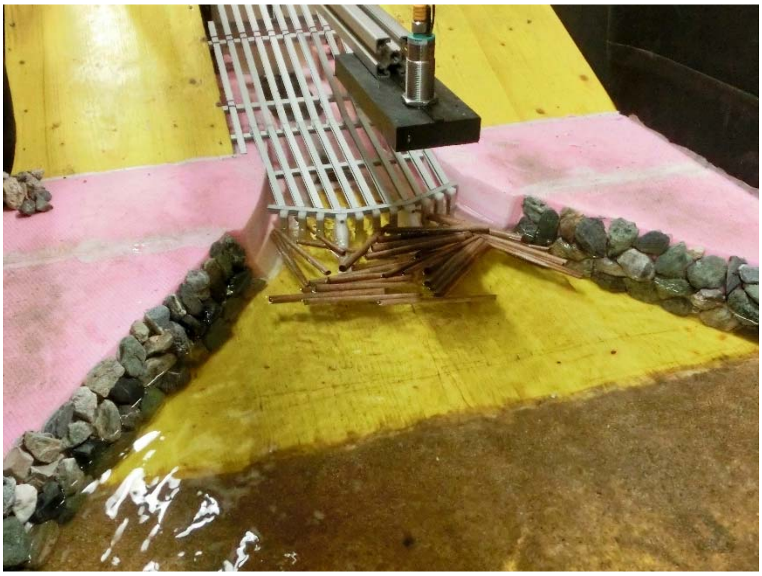

Figure 47: Woody debris in front of rake#4.

2.2.2 Effect of rake designs

The driftwood experiments show that all types of rakes filter the amount of driftwood, but rake#4 seems to be the most effective for the modeled scenario. It has to be noted, that these tests have been performed with an empty basin (no bedload deposition) and at a discharge, where no backwater effects are present. Rakes#2a, 3 and 4 are even more effective, when the basin is already prefilled, because then there is no more clearance between the ground and the rake.

2.3 Experiments with bedload transport

2.3.1 Setup

For the bedload experiments, the water and sediment supply for the model was redesigned. The channel started with a narrow 40 cm wide and 48 cm long channel, followed by a widening with an angle of 26° on both sides. This installation ensured a constant sediment transport. The installed conveyor belt provided the bedload material just above the model. In this way constant bedload transport could be guaranteed (see Figure 48).

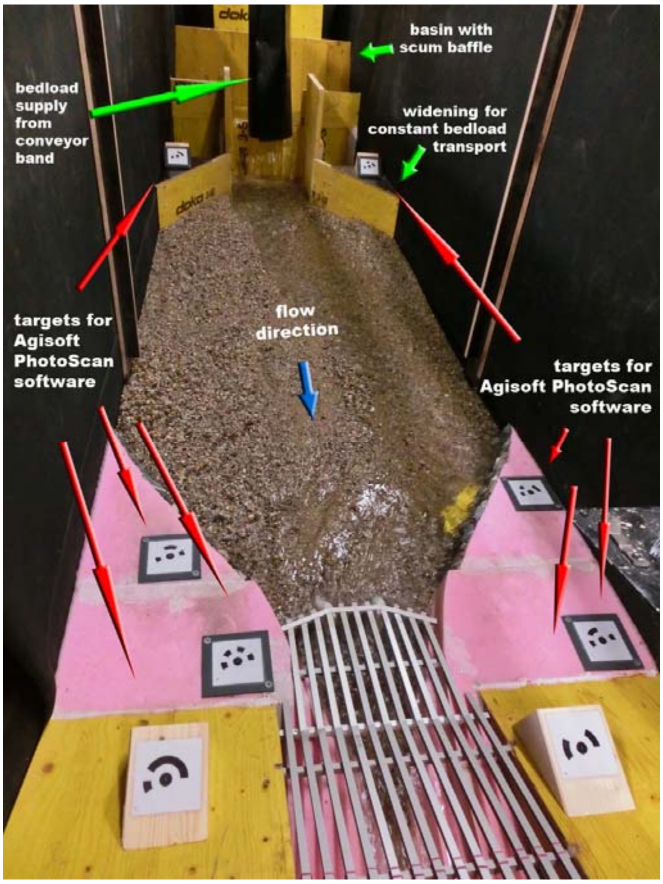

Figure 48: Retention basin with targets for photogrammetry and supply installation for the bedload experiments.

The sediment that passed the rake was transported easily through the outlet channel (see Figure 49). The round channel profile and the higher velocity in the parallel profile ensure that the material is flushed through and prevent logjams at the throttle.

Figure 49: Sediment transport after rake structure.

For the grain-size distribution of the added sediment, transect by number analyses provided by the Town of Canmore at Cougar Creek were evaluated after Fehr (1987) and downscaled for the physical scale of the model. The finest parts could not be considered for the physical model, because of the different behavior of cohesive material. A comparison of the downscaled grain-size distribution of the Cougar Creek and the sediment mixture used for the experiments is shown in Figure 50. The material has a density of 2.65 tons/m^3.

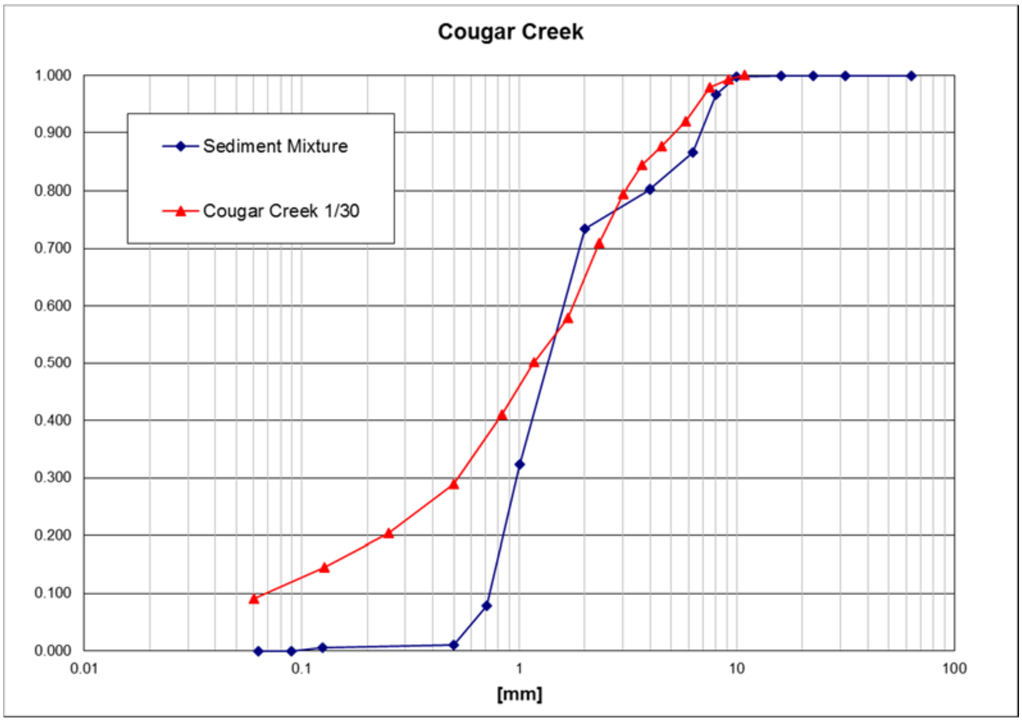

Figure 50: Comparison of the downscaled grain-size distribution and the sediment mixture used for the experiments.

2.3.2 Experiments

Different scenarios were modeled. First, the basin was filled with constant discharge (12 m^3/s natural scale) and bedload transport (0.14 m^3/s natural scale) until the bedload material reached the rake. Then stereoscopic pictures had generated an elevation model. The discharge was increased stepwise, first with and then without bedload addition. After each step an elevation model was generated and during the tests, sediment was trapped at the outlet of the outlet channel and evaluated for 1-minute intervals. Figure 51 to Figure 58 show the bedload transport experiments. The water discharge (blue line) and the sediment input (purple line) as well as the sediment output (magenta bars) are shown. The deposition volume in the basin based on the volumetric analysis is shown by hillshades. The related deposition volumes are shown in the diagrams.

2.3.2.1 Experimental run BL4

This run modeled a prefilled basin (until T=50min), followed by two smaller floods with additional bedload. The sequence ended with 5 flood peaks without sediment input to investigate the self-emptying behavior (all discharge values are given in Figure 52). For this experimental run all discharge rates could pass the throttle without backwater effects. After about 115 minutes sediment passed through the outlet channel. All sediment that passed the throttle was transported through the dam. During the whole experiment no material was deposited in the outlet channel.

Figure 51 shows the behavior of the deposited material. Until the time T=100min the basin was filled, then erosion was the dominant process.

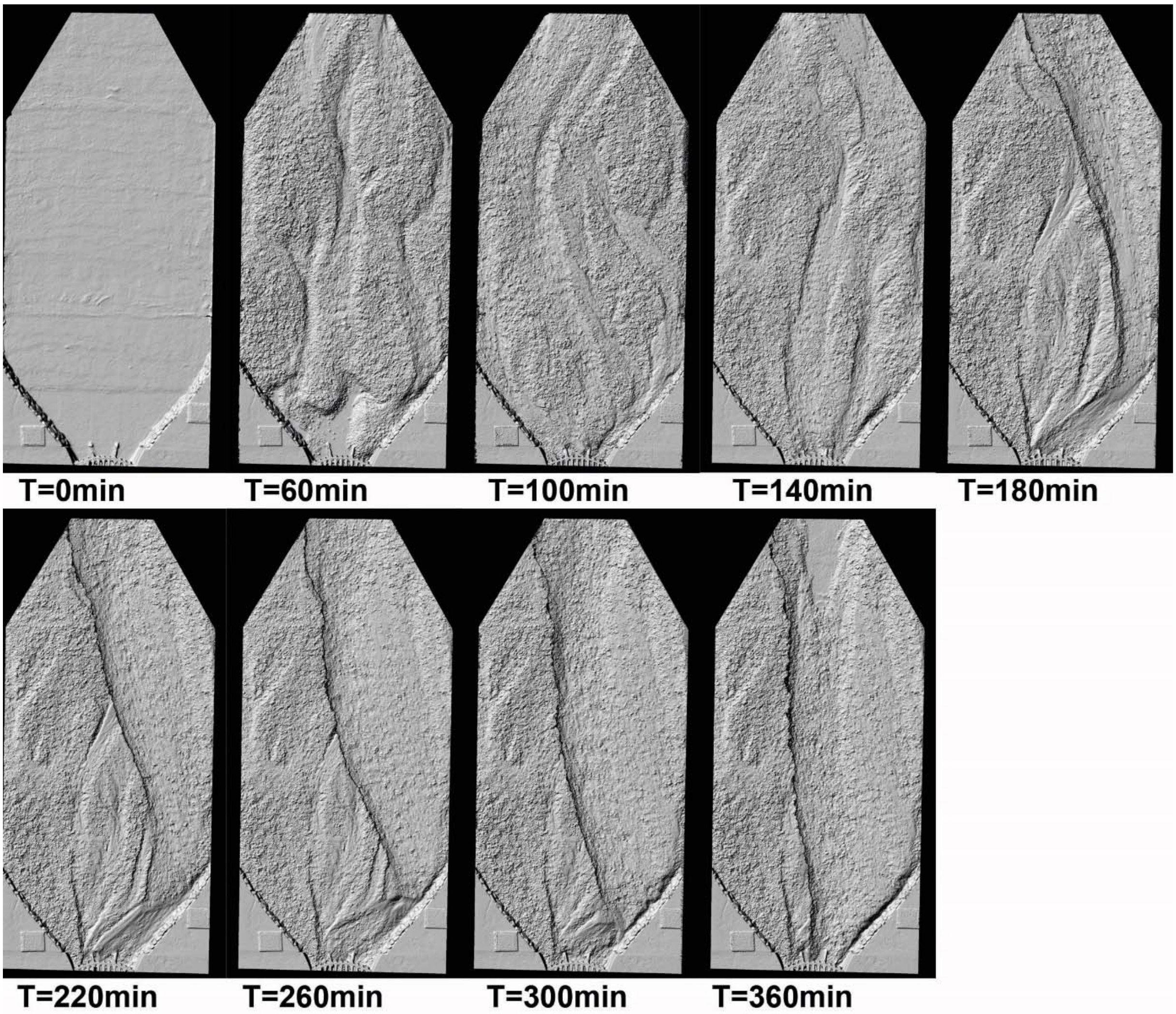

Figure 51: Hillshades of the bedload deposition at different times for the bedload transport experiment BL4.

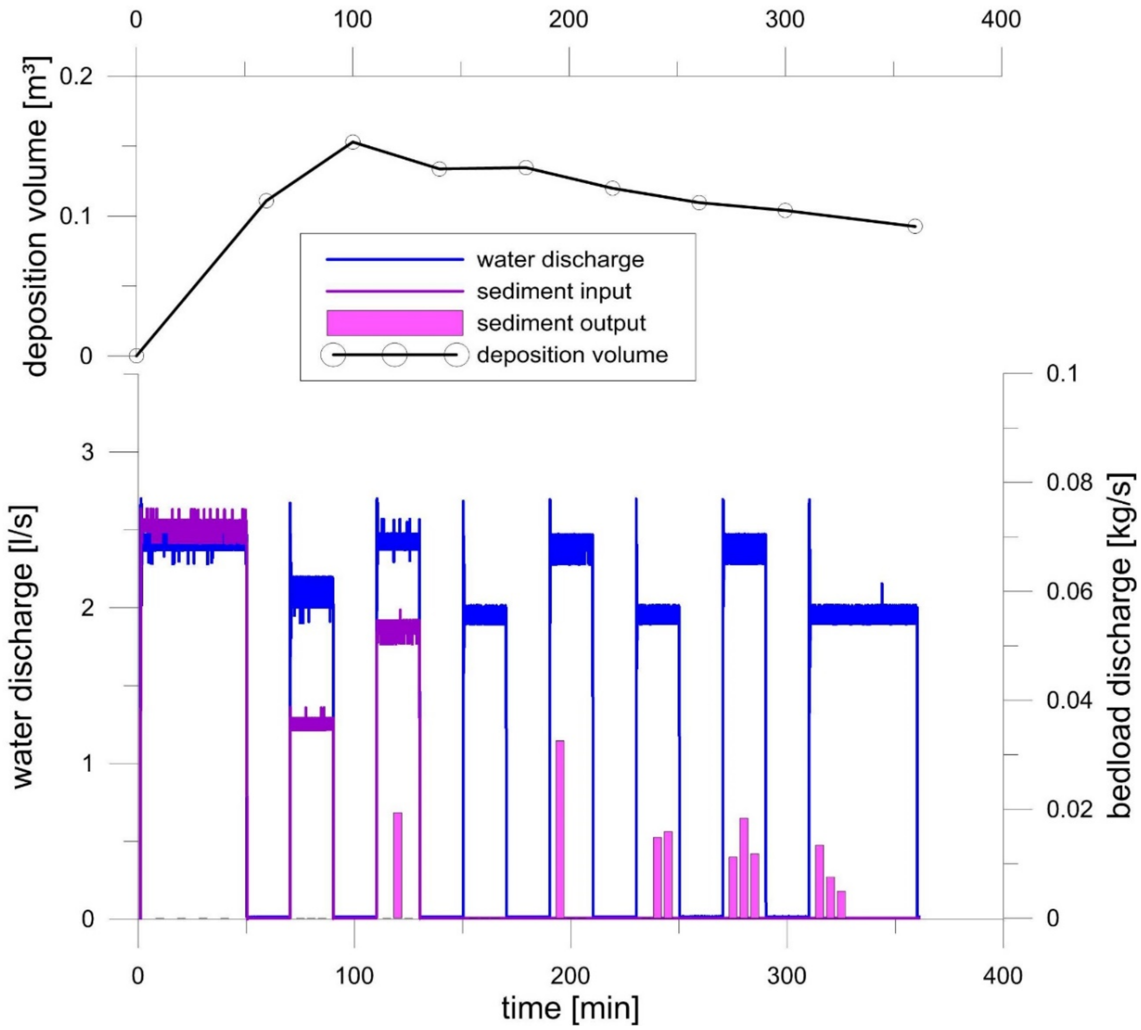

Figure 52: Water and sediment discharge for the bedload experiment BL4.

2.3.2.2 Experimental run BL5_6

This run modeled a prefilled basin (until T=60min), then a peak flow with additional bedload followed by a higher flood event. Another peak flow with additional bedload pursued the higher flood. During the higher flood backwater effects at the throttle were observed. During this time no material was transported through the outlet channel. When the discharge was reduced again no more backwater effects were present. At this stage sediment (T=250 min) transport through the outlet channel started again. All sediment that passed the throttle was transported through the dam. During the whole experiment no material was deposited in the outlet channel and deposition was the dominant process (compare: Figure 55 and Figure 56).

At the time T=150 min bedload material accumulated in front of the rake and the level of sediment was rising. Material was then deposited between the rake and the reach above the throttle.

Figure 53: Bedload transport through the throttle reduces 'maximum discharge'.

Figure 54: Throttle after suddenly stopped discharge.

This led to slightly reduced ‘maximum discharge’ conditions resulting in backwater conditions (see Figure 53). Due to the acceleration at the throttle, the throttle itself was never clogged during the experimental runs (see Figure 54).

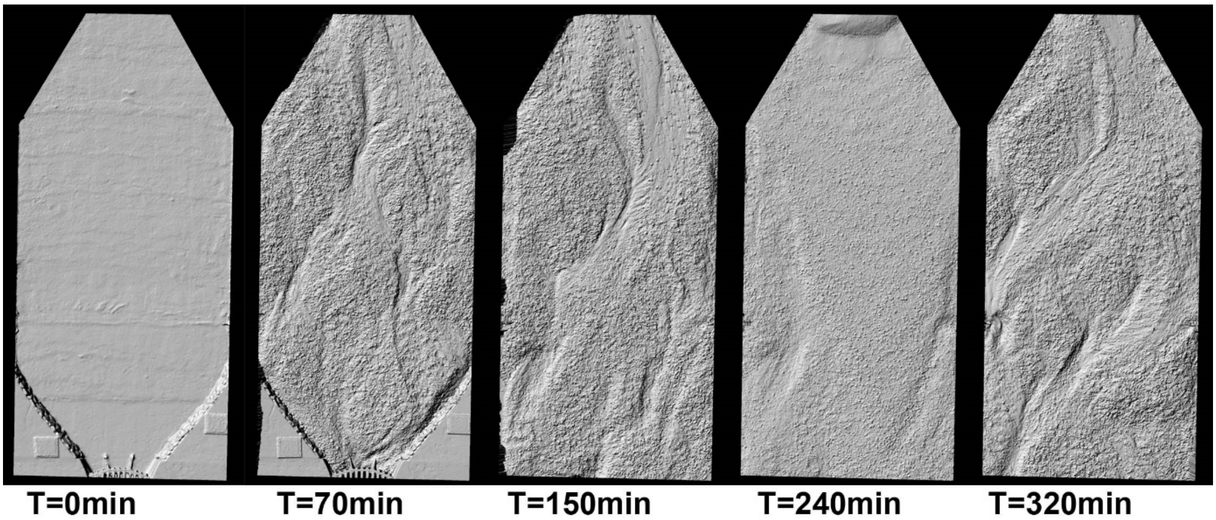

Figure 55: Hillshades of the bedload deposition at different times for the bedload transport experiment BL5_6.

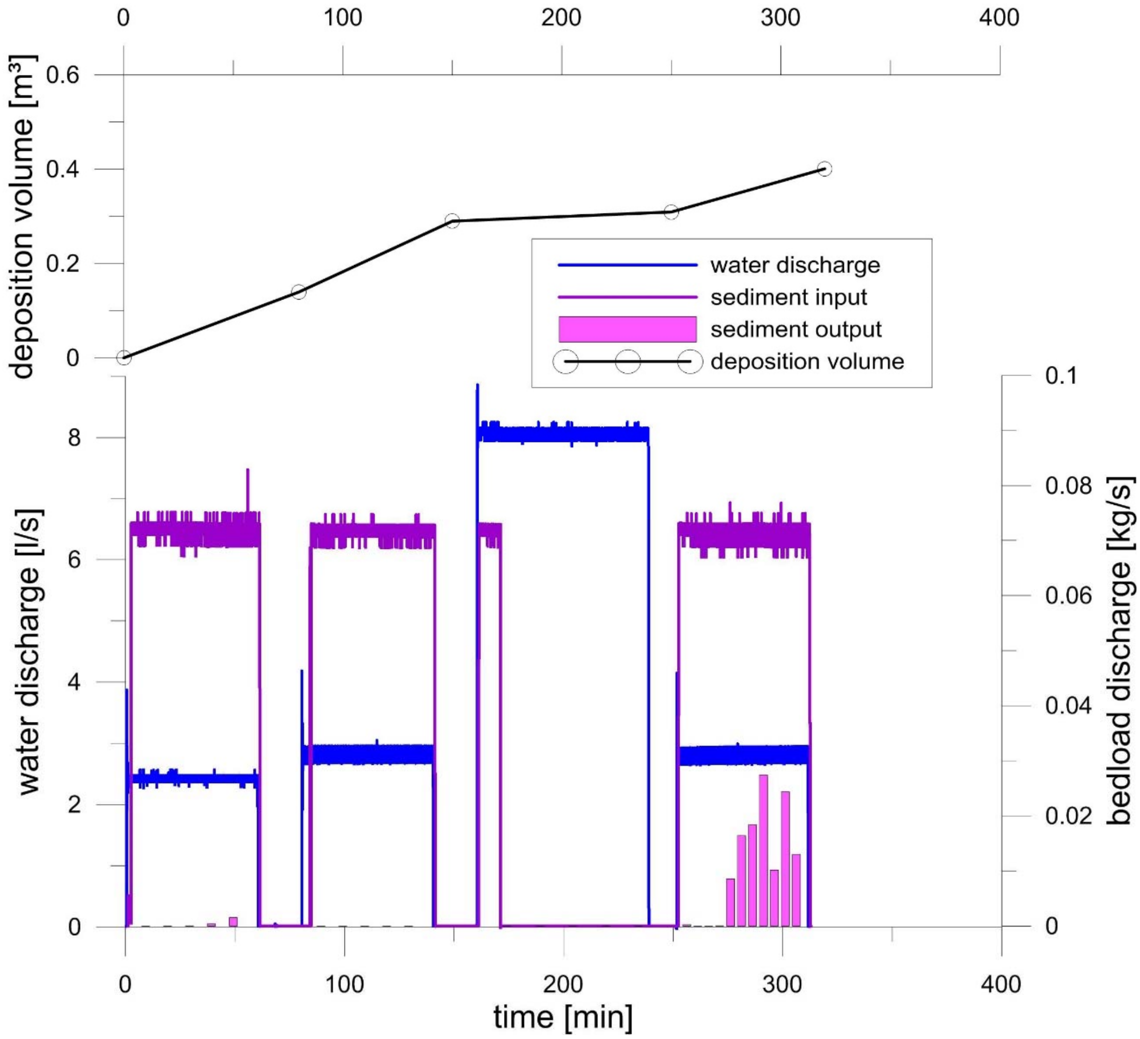

Figure 56: Water and sediment discharge for the bedload experiment BL5_6.

2.3.2.3 Experimental run BL7

The run modeled a prefilled basin (until T=60 min); then a short peak with additional bedload, followed by a smaller peak without sediment input. This was repeated three times. During the short, higher peaks, the backwater effects at the throttle were observed with no sediment passing the structure. The longer, lower peaks remobilized the deposited material. All sediment that passed the throttle was transported through the retention structure. During the whole experiment no material was deposited in the outlet channel.

Figure 57 shows the behavior of the deposited material. During the filling phase and the high discharge phases deposition was the dominant process. During the phases with lower discharge erosion took place in the basin (see Figure 58).

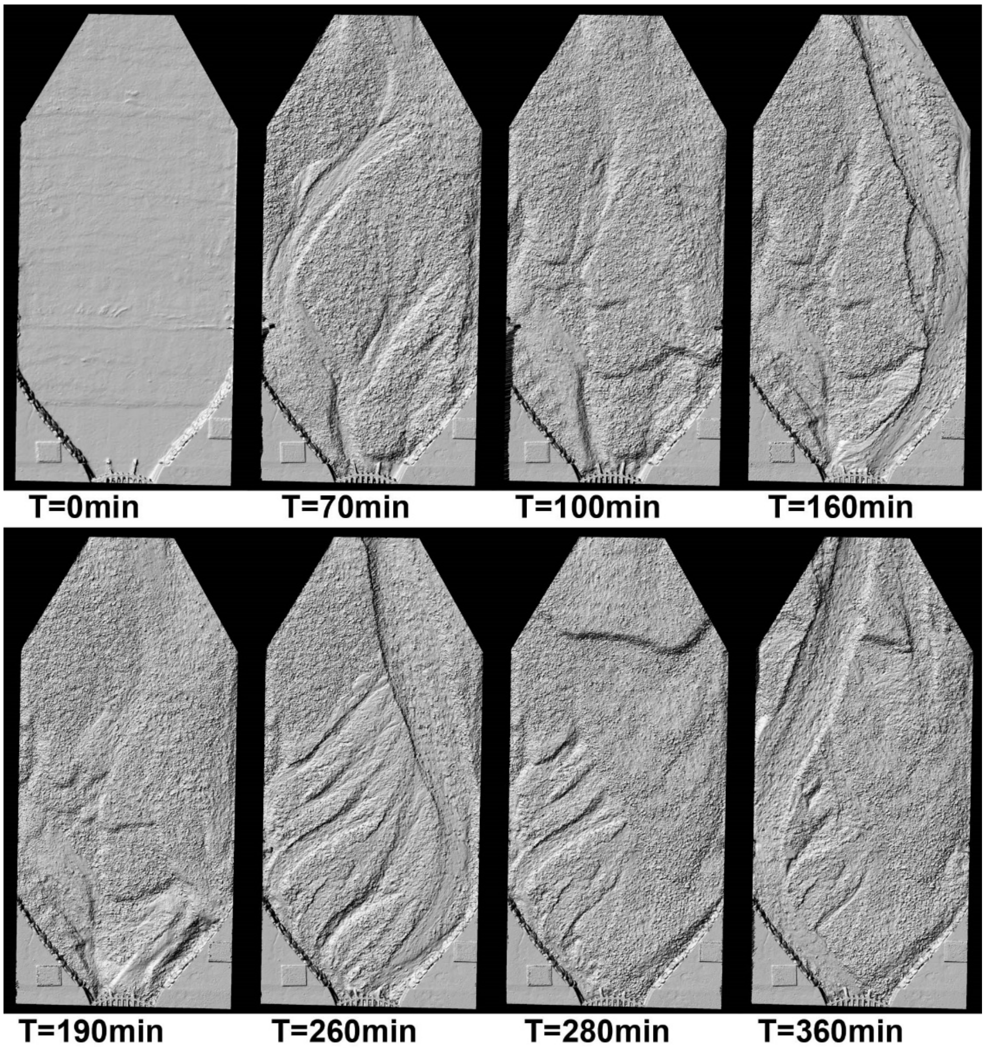

Figure 57: Hillshades of the bedload deposition at different times for the bedload transport experiment BL7.

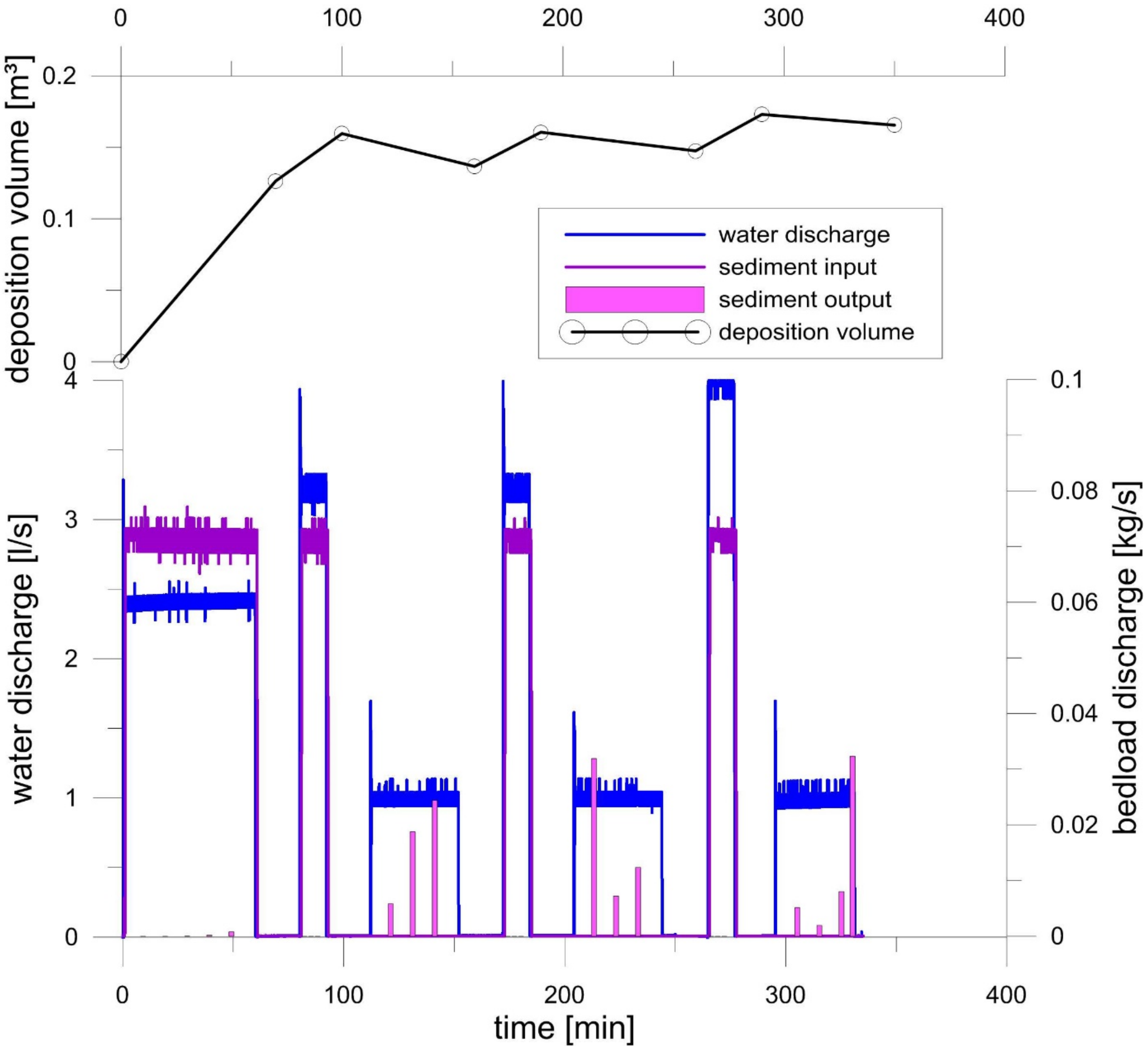

Figure 58: Water and sediment discharge for the bedload experiment BL7.

2.3.2.4 Effects in the stilling basin

The behavior of water and sediment in the stilling basin was documented with photographs.

There were some characteristic scenarios to observe:

- Discharges between 0 and 2.8 l/s (14 m^3/s) delivered bedload material to the stilling basin, which was then deposited. The higher discharges of this range also remobilized material in the stilling basin, in case of prefilled conditions. (compare Figure 59 and Figure 60)

- When the discharge exceeded 2.8 l/s, no bedload arrived at the stilling basin due to backwater effects on the other side of the structure. The increased discharge caused a remobilization of material (see Figure 61).

Figure 59: Deposited Material.

Figure 60: Depositing and remobilizing material.

Figure 61: Remobilizing material without sediment supply.

Figure 62: Discharge of 2.5 l/s (12 m^3/s in nature).

Figure 63: Discharge at 'full basin' conditions.

In Figure 62 the flow behavior at a discharge of 12 m^3/s is shown. Bedload deposition takes place in the not prefilled stilling basin. Figure 63 shows the same scenario, but under 'full basin' condition. The water of the outlet channel splash against the downstream wall of the stilling basin and no bedload transport can be observed.

2.4 Overflow scenario

For the overflow experiments, the downstream face of the dam structure was installed (see chapter 2.1.1.4). Several different setups were tested, including:

- flow dividers at the intersection of the embankment dam and the outlet structure for a ventilation of the channel;
- baffle blocks on the downstream boundary of the stilling basin to dissipate energy;
- chute and baffle blocks at the dam foot, to initiate a hydraulic jump close to the dam;
- different heights of the downstream boundary wall of the stilling basin;
- and different dimensions of the basin.

2.4.1 Velocity distribution

In order to get a velocity distribution over the downstream face of the dam (see Figure 64), a raster of measuring points, regularly spread over the area was used. The measuring was done using a flowmeter (see Figure 17 and Figure 65). At the lower quarter section of the dam entrapped air conditions over the whole width of the dam face were observed. Figure 64 shows the measured velocity distribution.

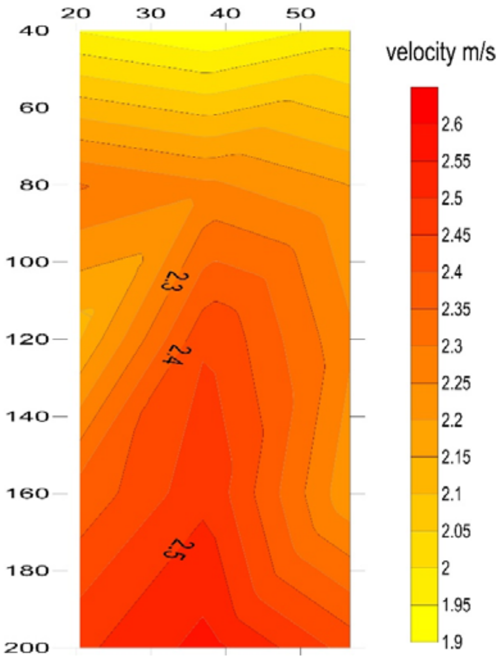

Figure 64: Measured velocity distribution.

Figure 65: Velocity measurements @ downstream dam surface.

2.4.2 Stilling basin

Figure 66 and Figure 67 show plots of the stilling basin, containing the installed chute and baffle blocks (grey). While the dam construction ended with the outlet of the channel for previous model runs, it was elongated for the investigations with overflow (lilac in Figure 66). Hence, the foot of the structure was located in the stilling basin. Parts of the chute and baffle blocks were integrated in the structure.

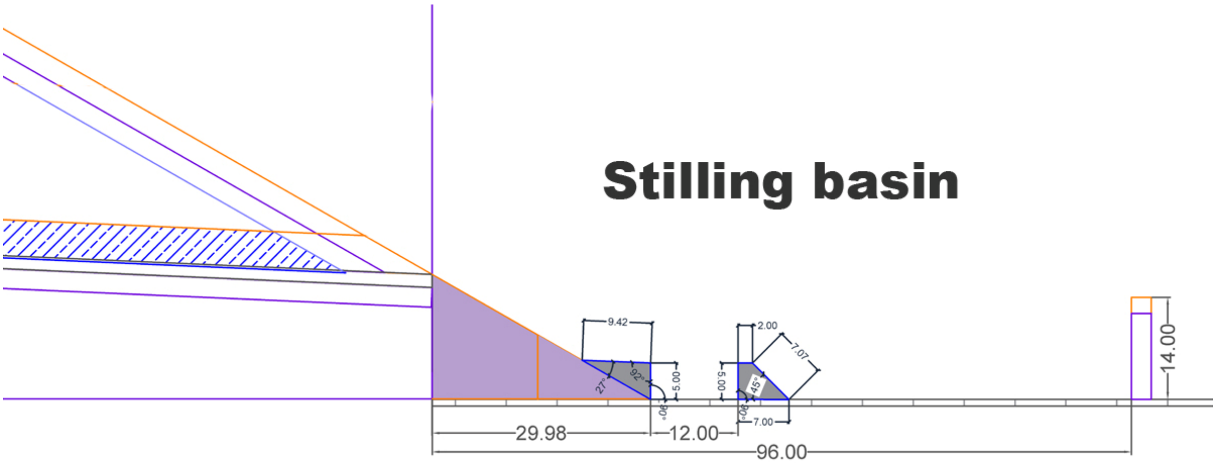

Figure 66: Longitudinal section of the stilling basin (dimensions in cm).

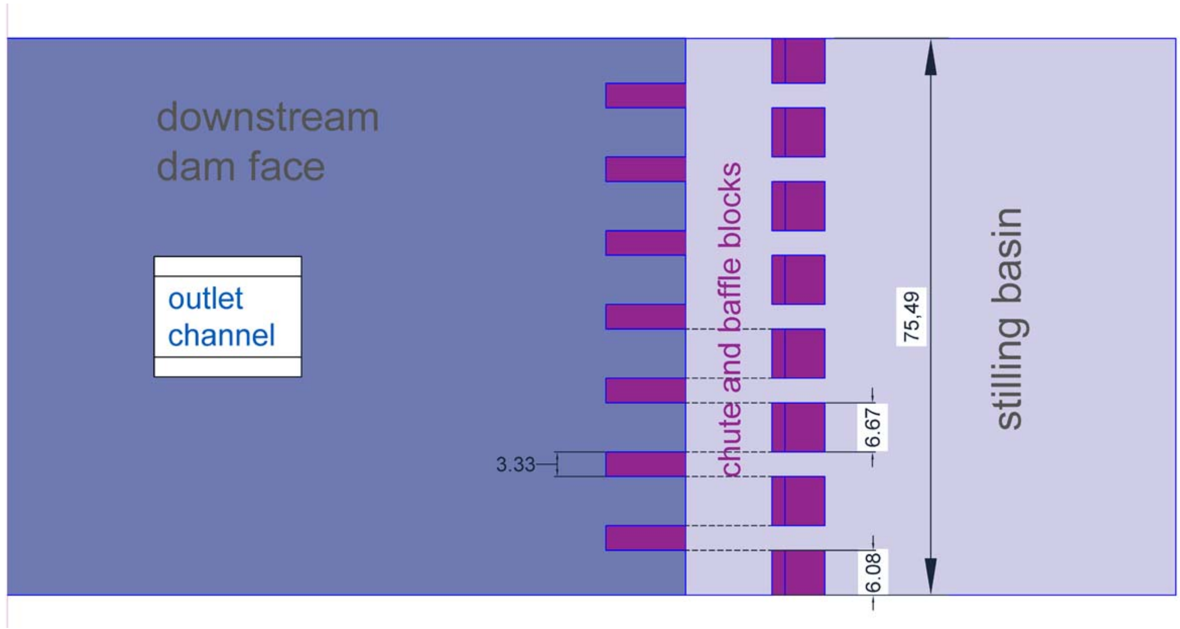

Figure 67: Ground plot of stilling basin, including chute and baffle blocks (dimensions in cm).

The effect of the blocks was the initiations of a direct hydraulic jump (see Figure 68), whereas the tests without blocks resulted in an elongated hydraulic jump (see Figure 69).

Figure 68: Stilling basin without chute and baffle blocks.

Figure 69: Stilling basin with chute and baffle blocks.

In Figure 70 it is possible to see the above-mentioned setup at ‘full basin’ conditions. In this case, the chute and baffle block structure is not effective and the main flow splashes in the basin and against the downstream boundary wall. Figure 71 shows the model on ‘overflow’ conditions; the chute and baffle blocks are activated resulting in a direct hydraulic jump (see Figure 71).

Figure 70: Stilling basin on 'full basin' conditions.

Figure 71: Stilling basin on 'overflow' conditions.

Experiments, where the stilling basin was prefilled with bedload material showed, that the sediment was washed out during the process of filling the retention basin (see Figure 72). While running the ‘overflow’ conditions, most of the sediment was remobilized, and a little remained in a vortex.

Behind the retention structure sedimentation patterns were observed during the emptying of the basin at the end of the ‘overflow’ scenario. The remaining material, which was not flushed out of the stilling basin, was relocated to the sides of the retention basin (see Figure 73).

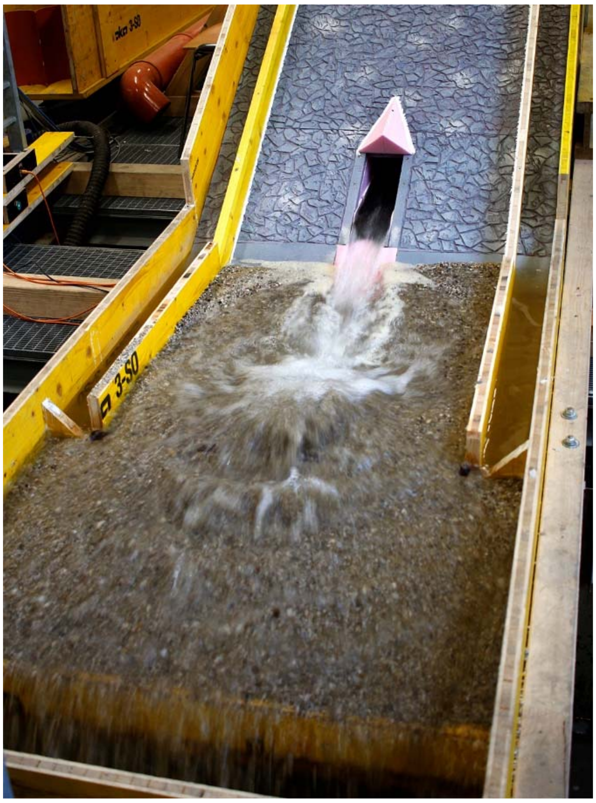

Figure 72: Starting a test with prefilled stilling basin.

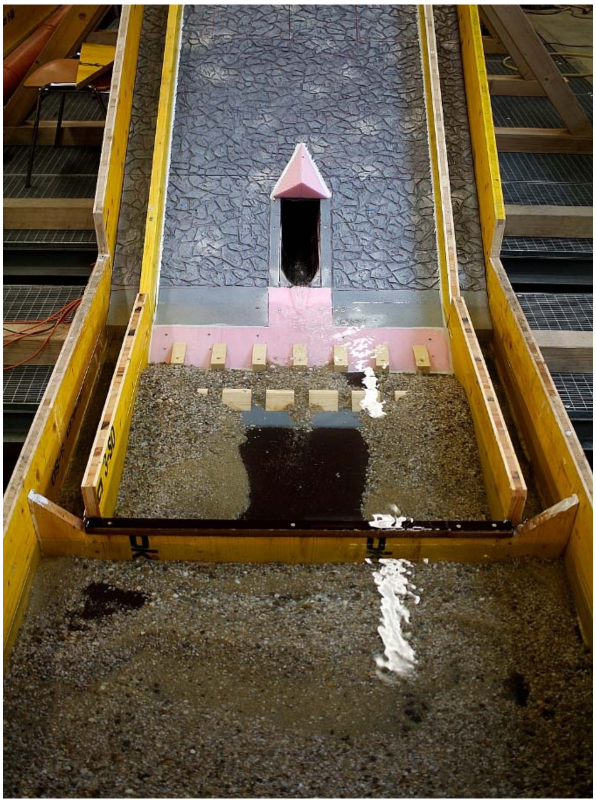

Figure 73: Erosion of Sediment after a 'overflow' test.

2.5 Investigations on the diversion tunnel

A second option for a bottom outlet of the debris flood retention structure was investigated within the detailed design phase. This option includes a mined diversion tunnel leading through the bedrock on the left side of the structure in combination with the spillway as defined in the base design.

The physical scale model was modified to test the hydraulic situation in the tunnel, including super elevation of the flow and impacts for the design of the aeration system. The scope of work included:

- Investigations on the required throttle opening height for the design of the diversion tunnel.
- Determination of the maximum free surface flow for the changed design.
- Velocity distribution along the longitudinal section of the diversion tunnel.
- Determination of super elevation in the tunnel.
- Investigations on the behavior of the sediment transport in the diversion tunnel.

2.5.1 Setup

The model as explained above was modified for the diversion tunnel. Because the diversion tunnel model was not integrated in the base model, the setup and measuring method is described in this chapter.

The given specifications for the diversion tunnel in natural scale were:

- An inner diameter of the diversion tunnel of 4.5 m.
- An inclination of 2.7 % over the longitudinal profile of the tunnel.
- An arc radius of the tunnel of 86 m at the center of the diversion tunnel.
- A tunnel length of 150 m.
- The same throttle shape as for the base design was used for the tunnel option with the lower edge in the horizontal position. The opening under the throttle leads to a semi-circular cross section.
- The storage level stays the same with 29.85 m water head at the lower edge of the throttle.
- A maximum discharge at 'full basin' conditions of 45 m^3/s.

For the physical scale model a horizontal platform was built on which a transparent flexible tube was placed in the specified dimensions and adjustment (see Figure 74).

From the intermediate basin a tubing transported the water to the diversion tunnel (flexible tube) with the throttle installed inside at the upstream end (see Figure 75). Tubes for pressure heights were connected to observe and control the pressure height. The diversion tunnel structure was fixed on a supporting profile with an inclination of 2.7% on the platform. Figure 76 shows a plan view of the tunnel model.

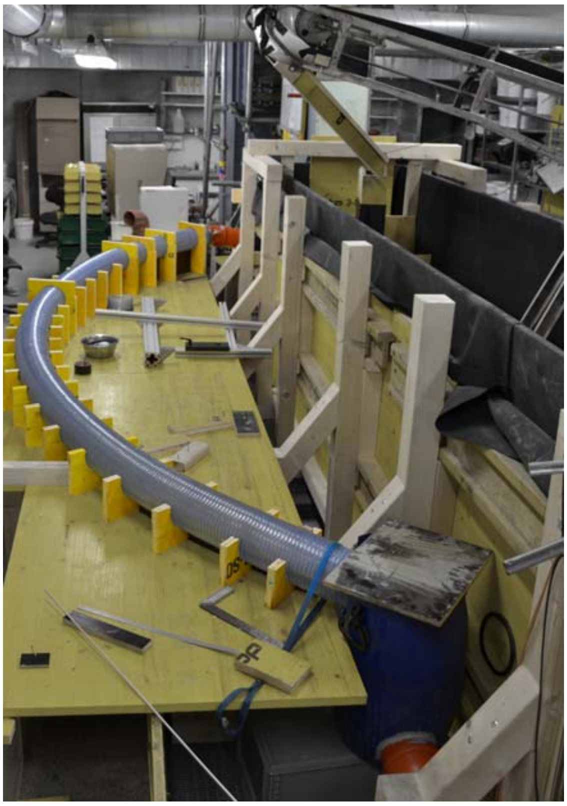

Figure 74: Platform and flexible tube of the diversion tunnel model.

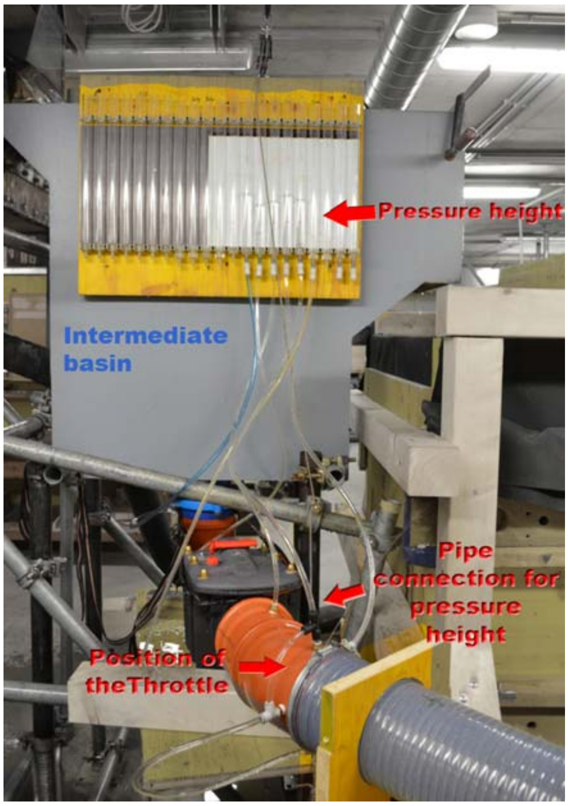

Figure 75: Water supply to the diversion tunnel model.

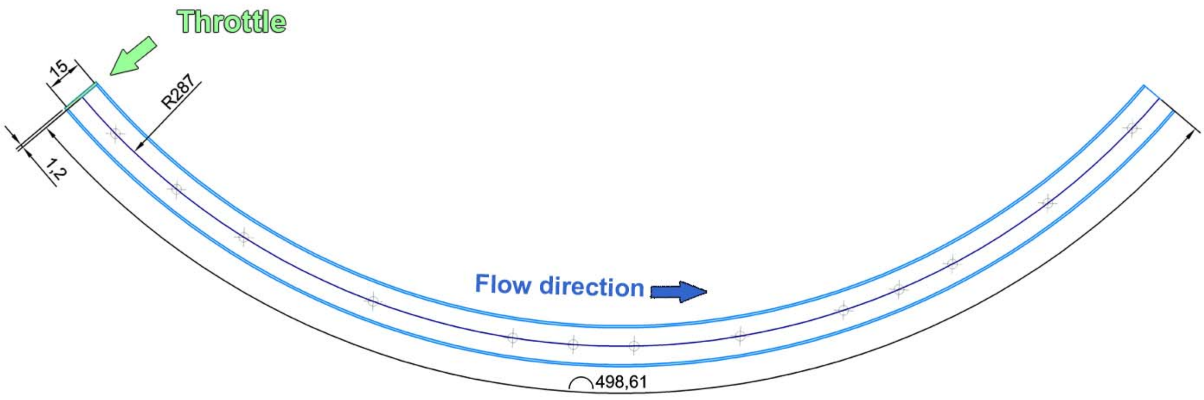

Figure 76: Plan view: diversion tunnel model (dimensions in cm).

2.5.2 Hydraulic investigation

2.5.2.1 Throttle opening height

For the hydraulic investigations, a 'full basin' experiment was performed to determine the specific throttle opening height for this design for a storage level of 29.85m in natural scale (99.5 cm in model scale). The test resulted in a throttle opening height of 3.7 cm in the model (1.11 m natural scale).

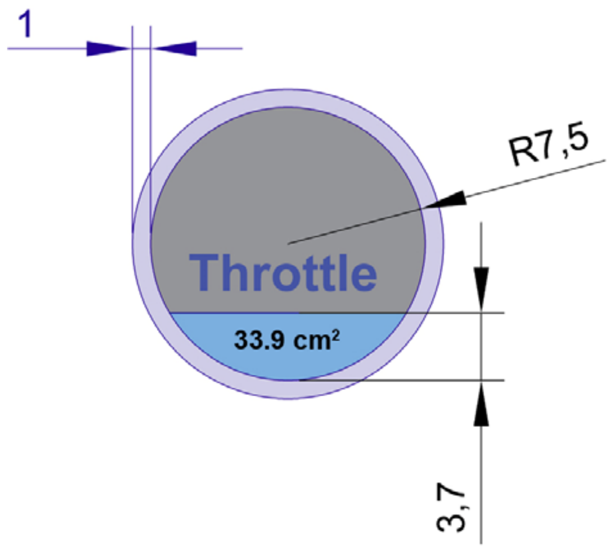

Figure 77: Cross section of the diversion tunnel model at the throttle (undefined dimensions in cm).

2.5.2.2 Maximum free surface flow

The opening area at the throttle changed from 33.15 cm^2 in the previous model to 33.9 cm^2 (2.98 m^2 to 3.05 m^2 natural scale). The effect of this deviation in the model is within the measuring tolerance. Thus, it is assumed that the maximum free surface flow will be the same for the base design and the diversion tunnel, as long as the inlet has the same inclination and hydraulically convenient shape.

2.5.2.3 Super elevation

For the super elevation investigations, the discharge in the model was set to 9.13 l/s (45 m^3/s in natural scale). The transparent tube allowed to trace the water height at the longitudinal section at the inner and outer radius of the diversion tunnel. The pictures in Figure 78 show the flow condition at the specific discharges at the position of the highest super elevation. The so created lines were measured and projected to the center radius of the tunnel, as can be seen in Figure 80.

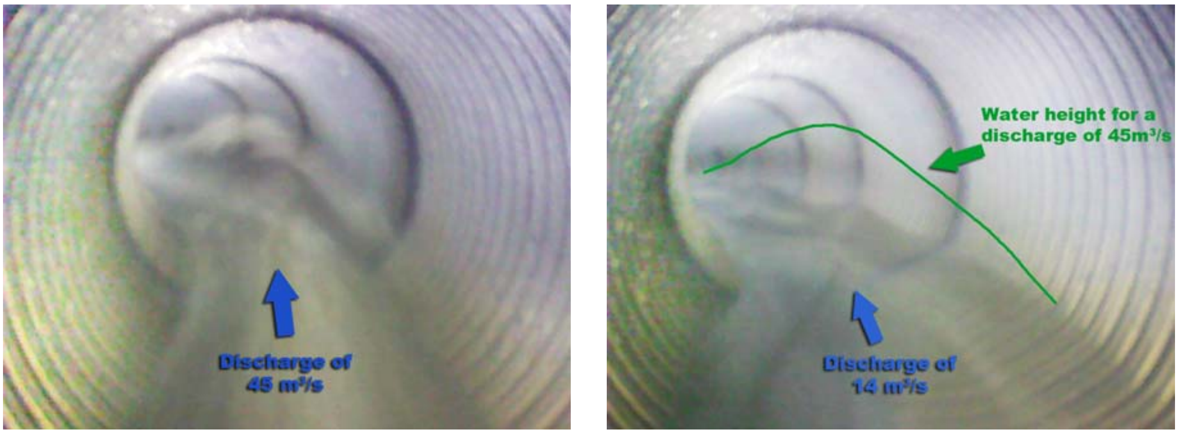

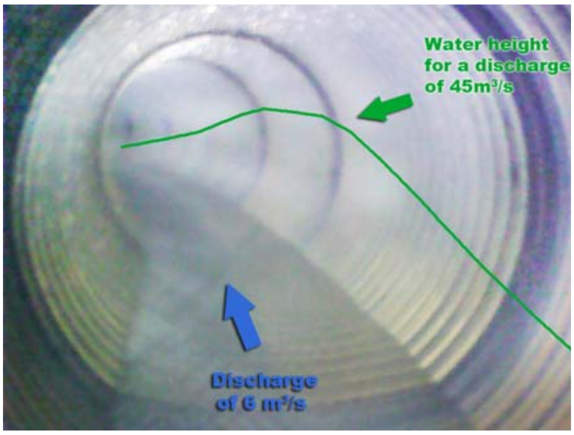

Figure 78: The point with the highest value of super elevations at the stated discharges (natural scale).

At steady state conditions with a discharge of 9.13 l/s model scale (45 m^3/s natural scale), the point of the highest super elevation was reached at 88 cm downstream of the throttle in the model (26.4 m natural scale). Later in the flow the super elevation decreased. At 175 to 214 cm (52.5 to 64.2 m in naturals scale) downstream of the throttle the super elevation was about zero, and increased again to a second peak at 262 cm (78.6 m natural scale) and a third one at 398 cm (119.5 m natural scale) downstream of the throttle. The values for this peaks in natural scale are shown in Table 8.

Table 8: Values for the three peaks of the super elevation in natural scale.

Position downstream of the throttle [m]	Water height at the outer radius [m]	Water height at the inner radius [m]	Super elevation [m]
26.3	3.5	0.4	3.1
78.7	3.2	0.6	2.6
119.5	2.4	0.9	1.6

2.5.2.4 Energy heights

Experiments to investigate the energy heights in the diversion tunnel were run at 'full basin' conditions (45 m^3/s discharge in natural scale) to get information about the worst case scenario. Observations on the hydraulic conditions in the tunnel was done at 16 locations. These were located at the main points of interest, like the highest and lowest points of the super elevation, the upstream end of the tunnel, directly at the throttle, upstream of the throttle and at the half distance in between the points of the highest and lowest super elevation. The measuring positions of the tunnel model are shown in Figure 76.

At these locations the water heights were measured by a metal stick measuring the distance from the upper edge of the tunnel to the water surface under different angles. To gain the information about the water surface, these data were imported to AutoCAD and processed to see the different forms of water surface. The points of the highest and lowest water elevation are shown in the upper diagram of Figure 80. The corresponding flow area (comparable to flow conditions without super elevations) was calculated to determine the different velocities and pressure heights.

After Bernoulli the total Energy head E can be calculated for every measured cross-section:

$$E = z + y + \frac{v^2}{2g}$$

Where z is the elevation of the channel, y is the flow depth and $v^2/2g$ is the velocity head with v being the velocity (see Figure 79).

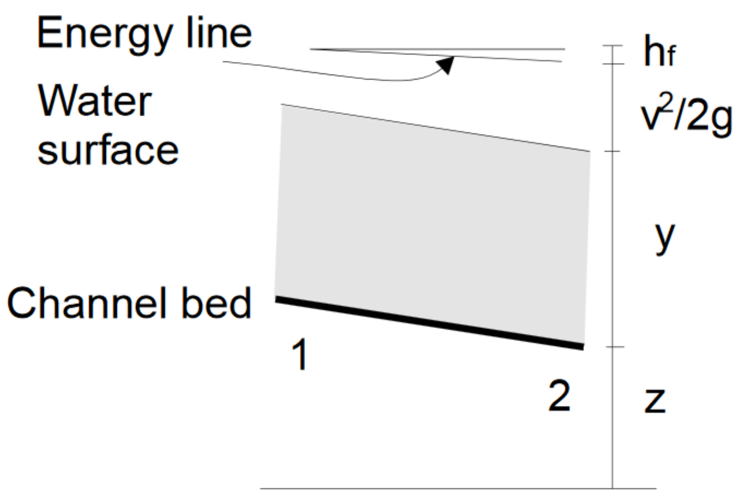

Figure 79: Energy line for open channel flow (from CIVE2400 2008).

With increasing distance from the throttle it was possible to observe decreasing velocity and energy height (see lower diagram at Figure 80).

Table 9 shows the calculated velocity for the certain positions. As can be seen in Table 9 and Figure 80 (Energy grade line diagram) there are rising values at the positions of the highest super elevations. This effect can be attributed to entrapped air, which may falsify the measurement at this positions.

Table 9: Velocity distribution at the longitudinal section of the diversion tunnel in natural scale.

Distance from throttle [m]	Calculated velocity [m/s]
-3	2,83
0	24,61
6,049	22,00
16,158	19,31
26,268	19,85
43,931	17,36
61,594	15,57
69,020	14,90
76,446	15,58
89,466	14,25
102,486	14,09
109,727	14,18
116,969	14,43
130,798	12,54
144,628	12,30

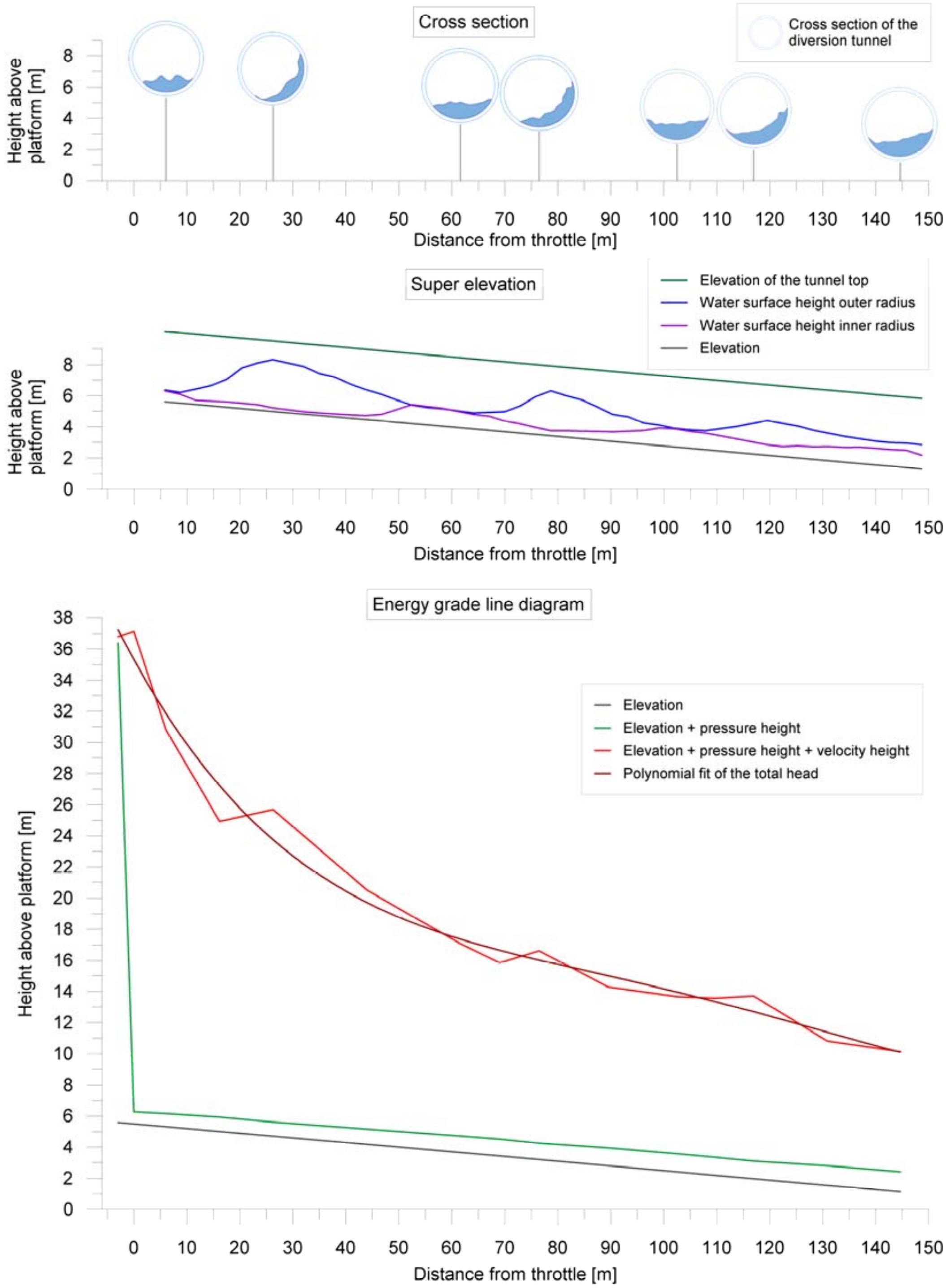

Figure 80: Diagram including cross sections, super elevation and the energy grade lines at the longitudinal profile of the diversion tunnel (values in natural scale).

2.5.3 Sediment transport investigation

To explore a possible sediment deposition in the diversion tunnel, experiments with sediment were made. The base design experiments showed a maximum sediment transport of 0.032 kg/s in model scale (see Figure 58), what correspond to 0,06 m^3/s in natural scale. For the investigations on the diversion tunnel model this 0.032 kg/s were used for tests with discharges from 1.2 to 9.13 l/s (6 to 45 m^3/s natural scale): The grain size distribution of the sediment was the same as in the 'experiments with bedload transport', the input position was just downstream of the throttle.

The experiments showed that all the sediment was transported through the tunnel and no sedimentation within the tunnel was registered at all tested discharges. Figure 81 and Figure 82 show the sediment transport at the end of the tunnel at the stated discharges.

Figure 81: Sediment transport at 6 m^3/s natural scale.

Figure 82: Sediment transport at 14 m^3/s natural scale.

3 Conclusions and Recommendations

3.1 Hydraulic experiments

With the 'full basin' experiment, an throttle opening height of 4.3cm, respectively 1.3m in real scale was determined for the round channel design with an diameter of 3 m in real scale.

For this throttle opening the 'maximum discharge' test showed a discharge of 2.75 l/s, which means $13.6m^3/s$ for real conditions, that can pass the retention structure without backwater effects.

The throttle design (45° versus straight edge) did not influence the discharge significantly.

None of the tested rake type influenced the discharge through the structure at 'full basin' conditions. The 'maximum discharge' was not influenced by the rake as long as the distance between the rake and throttle was sufficient. If the rake structure, independent from the design, was installed too close to the area of flow acceleration, first backwater effects at the throttle could be observed at smaller discharges.

The rakes with horizontal beams at the lower level of the rake (Rake#2a and Rake#3) increased the backwater effect of the rake slightly at the most upstream measuring position. Below the rake structure, there was no significant influence of the rake on the flow conditions.

When the retention structure was filled with water, up to the dam crest, and the throttle opening was 1.3 m, the velocity in at the lower part of the outlet channel was around 16 m/s. The nappe showed a distance from 4.5 m to 11.4 m from the end of the outlet channel. These distances were measured on the height of the downstream wall crest.

3.2 Experiments with woody debris

The driftwood experiments showed that all tested types of rakes reduce the amount of driftwood by at least 90%, but rake#4 seems to be most effective for the modeled scenario. It has to be noted, that these tests have been performed with an empty basin (no bedload deposition) and at a discharge with no backwater effects. Rakes#2a, 3 and 4 are even more effective, when the basin is already prefilled, because then there is no more or smaller clearance between the ground and the rake. As soon as backwater effects are present it is very unlikely that driftwood passes the rake, because of the reduced flow velocity in front of the rake.

3.3 Experiments with bedload transport

3.3.1 Deposition behavior and remobilization of material

For the experiments starting with empty basin conditions the bedload layer had to reach the rake first, and then the material was partly transported through the rake and passes the throttle (under natural conditions sediment is available immediately). As soon as backwater effects were present all added material was deposited in the basin. When normal flow conditions were reached again (no backwater at the throttle) the deposited material was remobilized again. Without additional bedload, erosion was the dominant process in the deposition basin.

3.3.2 Bedload transport in the outlet channel

In none of the experiments deposition in the outlet channel took place. All material that passed the throttle was transported through the dam. For the case of high bedload transport and starting backwater conditions material was deposited between the rake and the reach above the throttle. Due to the acceleration at the throttle, the throttle itself had never been clogged during the experimental runs.

3.3.3 Bedload deposition/erosion behavior in the ‘stilling basin

Experiments, where the stilling basin was prefilled with bedload material showed that deposition takes place at discharges from 0 to 13,6m^3/s (‘normal flow’ conditions). Higher discharges of this range also caused a remobilization of sediment, when the basin was completely filled up with sediment. Discharges higher than 13,6m^3/s (showing a water retention upstream the dam) led to mobilization of sediment in the retention basin. While running the ‘overflow’ conditions, most of the sediment was remobilized, and a little remained in a vortex. During the emptying of the retention basin following the ‘overflow’ scenario, the remaining material was moved to the sides of the retention basin.

3.4 Overflow

The experiments showed that the tested chute and baffle blocks are very effective. The chute and baffle blocks initiated a direct hydraulic jump in the first sector of the stilling basin during ‘overflow’ conditions, whereas the tests without blocks resulted in an elongated hydraulic jump. But in the case of ‘full basin’ conditions, the chute and baffle block structure was not effective and the main flow splashed in the stilling basin and against the downstream boundary wall.

3.5 Diversion tunnel option

A second option for the bottom outlet was specified as a diversion tunnel leading through the bedrock on the side of the structure. The tunnel in natural scale has a diameter of 4.5 m, an inclination of 2.7 %, a radius of 86 m and a length of 150 m.

For this setup, a throttle opening height of 1.11 m natural scale was detected, the maximum free surface flow was the same as in the tests with the outlet channel (13.6 m^3/s natural scale).

The super elevation reached a maximum of 3.1 m, 26.2 m (natural scale) downstream of the throttle. At this position the water height in the diversion tunnel at the outer radius is 3.5 m (natural scale) over the tunnel bottom. The water did not reach the top of the tunnel.

The natural scale velocity range was calculated with 24.6 m^3/s (highest value) at the throttle to 12.3 m^3/s (lowest value) at 144.6 m downstream of the throttle.

Investigations with bedload transport show no deposition of sediment in the diversion tunnel for the tested setup.

3.6 Scaling issues in hydraulic modelling

According to Taveira Pinto (2012) differences between the model and the prototype behavior may occur due to several reasons; however:

- Scale effects are always present.
- The bigger the scaling factor, the larger will be the scale effects.
- Scale effects do not affect all phenomena/parameters under investigation in the same way – qualitatively they may be reproduced differently between model and prototype, but quantitatively they can be properly scaled (discharge vs air entrainment).
- In general some parameters are smaller in the model than in prototype – relative wave height, relative discharge, transported relative volume of sand, etc.

Froude similarity is normally considered in open-channel hydraulics, where friction effects are negligible (deep-water wave propagation) or for highly turbulent phenomena, since the energy dissipation depends mainly on the turbulent shear stress terms. Statistically, these are correctly scaled even though the turbulent fine structures and the average velocity distribution differ between the model and prototype flows. The gravitational acceleration is not scaled as well as the other numbers.

Therefore up-scaled model results have to be interpreted carefully.

4 References

ALPINFRA CONSULTING + ENGINEERING GMBH (2015). Mountain Creek Hazard Mitigation, Design of mitigation measures, Cougar Creek. Interim Report 03: Final Option Analysis. Dated from January 2015.

BGC ENGINEERING Ltd. (2014). Cougar Creek debris flood hazard assessment. Final report revised prepared for the Town of Canmore. Dated from June 2014.

CANMORE (2015a). About Canmore, Mountain Creek Hazard Mitigation. *In*: The Town of Canmore [online]. Date of consulting: 18/08/2015. Available on: http://www.canmore.ca/

CANMORE (2015b). Cougar Creek long-term mitigation, Option analysis summary report. Cougar Creek Option Selection. Dated from January 2015.

CIVE2400 Fluid Mechanics (2008). Section 2: Open Channel Hydraulics by Dr Goodwill and Dr Sleigh, University of Leeds, School of Civil Engineering.

PEPPERL + FUCHS GROUP, 2014. Ultrasonic sensor UC500-30GM-IUR2-V15. Instructions.

PREIßLER G. and BOLLRICH G. (1985). Technische Hydromechanik/1. Verlag für Bauwesen, Berlin, 2nd Edition. Pages 299 and 500 to 505.

Preissler, G.; Bollrich, G.; Martin, H. (1989): Technische Hydromechanik. Band 2: Spezielle Probleme. Berlin: Verlag Bauwesen

ROCKWELL AUTOMATION Inc. (2015). Ultrasonic Advantages and Disadvantages. *In*: Rockwell Automation Inc. [online]. Date of consulting: 15/07/2015. Available on: http://www.ab.com/

TAVEIRA PINTO F. (2012): Scaling Issues in Hydraulic Modelling, Date of consulting 7/06/2016. Available on: http://www.coastalwiki.org/wiki/Scaling_Issues_in_Hydraulic_Modelling

5 Attachments

Test protocols and Video sequences are provided in a separated document.